

CHOMP: Multimodal Chewing Side Detection with Earphones

JONAS HUMMEL* and MAXIMILIAN BURZER*, Karlsruhe Institute of Technology, Germany

FELIX SCHLOTTER, Karlsruhe Institute of Technology, Germany

MICHAEL KÜTTNER, Karlsruhe Institute of Technology, Germany

TOBIAS KING, Karlsruhe Institute of Technology, Germany

QIANG YANG, University of Cambridge, United Kingdom

CECILIA MASCOLO, University of Cambridge, United Kingdom

MICHAEL BEIGL, Karlsruhe Institute of Technology, Germany

TOBIAS RÖDDIGER, Karlsruhe Institute of Technology, Germany

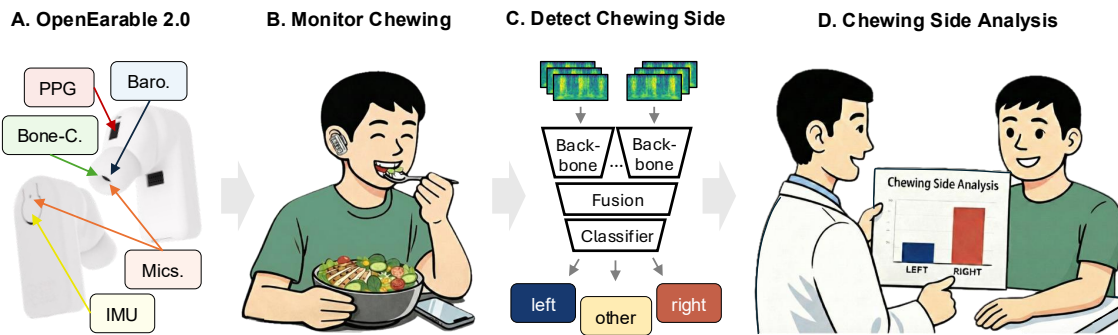


Fig. 1. CHOMP Pipeline: A. Two OpenEarable 2.0 devices are employed to collect data from five sensing modalities.; B. A user wearing OpenEarable 2.0 devices during a meal while chewing activity is recorded.; C. Windowed sensor signals are transformed into scalograms using the Continuous Wavelet Transform and processed by a chewing-side classifier.; D. A dentist discussing the results of the analysis with his patient.

Chewing side preference (CSP) has been identified both as a risk factor for temporomandibular disorders (TMD) and behavioral manifestation. Despite TMDs affecting roughly one third of the global population, assessment mainly relies on clinical examinations and self-reports, offering limited insight into everyday jaw function. Continuous CSP monitoring could provide an objective proxy for functional asymmetries. Prior wearable approaches, however, mostly use specialized form factors and demonstrate limited performance. We therefore present CHOMP, the first system for chewing side detection using earphones. Employing OpenEarable 2.0, we collected data from 20 participants with microphones, a bone-conduction microphone, IMU, PPG, and a pressure sensor across eleven foods, five non-chewing activities, and three noise conditions. We apply the Continuous Wavelet Transform to each sensing modality and use the resulting multi-channel scalograms as inputs to CNN-based classifiers. Microphones achieve the strongest single-sensor unit performance, with median F_1 scores of 94.5% in leave-one-food-out (LOFO) and 92.6% in leave-one-subject-out (LOSO) cross-validations. Fusing sensing modalities further improves performance to 97.7% for LOFO and 95.4% for LOSO, with additional evaluations under noise

*Both authors contributed equally to this research.

Authors' Contact Information: [Jonas Hummel](mailto:jonas.hummel@kit.edu), jonas.hummel@kit.edu; [Maximilian Burzer](mailto:maximilian.burzer@kit.edu), maximilian.burzer@kit.edu, Karlsruhe Institute of Technology, Karlsruhe, Germany; [Felix Schlotter](mailto:upsxl@student.kit.edu), upsxl@student.kit.edu, Karlsruhe Institute of Technology, Karlsruhe, Germany; [Michael Küttner](mailto:michael.kuettner@kit.edu), michael.kuettner@kit.edu, Karlsruhe Institute of Technology, Karlsruhe, Germany; [Tobias King](mailto:tobias.king@kit.edu), tobias.king@kit.edu, Karlsruhe Institute of Technology, Karlsruhe, Germany; [Qiang Yang](mailto:qiang.yang@cl.cam.ac.uk), qiang.yang@cl.cam.ac.uk, University of Cambridge, Cambridge, United Kingdom; [Cecilia Mascolo](mailto:cm542@cam.ac.uk), cm542@cam.ac.uk, University of Cambridge, Cambridge, United Kingdom; [Michael Beigl](mailto:michael.beigl@kit.edu), michael.beigl@kit.edu, Karlsruhe Institute of Technology, Karlsruhe, Germany; [Tobias Röddiger](mailto:tobias.roeddiger@kit.edu), tobias.roeddiger@kit.edu, Karlsruhe Institute of Technology, Karlsruhe, Germany.

interference indicating robust performance. Our results establish earphones as a practical platform for continuous CSP monitoring, enabling clinicians and patients to assess jaw function in everyday life.

CCS Concepts: • **Human-centered computing** → **Ubiquitous and mobile computing**; • **Applied computing** → *Health care information systems*; • **Hardware** → Sensors and actuators; • **Computing methodologies** → Machine learning.

Additional Key Words and Phrases: Chewing Side Preference, Temporomandibular Disorders, Earphones, True Wireless Stereo, Earables, Multimodal Sensing

1 Introduction

Chewing side preference (CSP) describes the habitual tendency to chew predominantly on one side of the jaw [34, 72]. It has been shown to be both a risk factor [8, 84] for developing temporomandibular disorders (TMDs) and a behavioral manifestation observed in patients with existing TMDs [47, 89]. TMDs are present in approximately one third of the global population [4, 91]. Accordingly, at the beginning of the last decade, annual treatment and management costs were already estimated at USD 4 billion in the US alone [56]. Despite their prevalence, TMDs are primarily diagnosed and monitored through self-reports and clinical examinations [20, 54], providing limited insight into patients' everyday functional condition and constraining opportunities for early prevention. This lack of objective, longitudinal data highlights the potential of wearable approaches that can be seamlessly integrated into daily life, thereby capturing chewing behavior under naturalistic conditions.

Wearable solutions for chewing side detection have been proposed, including surface EMG electrodes [88], a combination of microphones positioned around the face [19, 51, 52], a headband [87] and glasses [15]. While these approaches demonstrate the potential of wearable solutions to solve the problem, all but the latter rely on form factors not commonly worn in everyday life. In contrast, earphones are widely adopted and socially accepted, mainly in the form of the now commercially dominant true wireless stereo (TWS) earphones. Positioned in close proximity to the temporomandibular joint, earphones can capture multiple chewing-related signals, including masseter muscle motion via inertial sensing [16], chewing acoustics via microphones [35], and subtle ear canal deformations reflected in pressure changes [6], making them particularly well-suited for chewing side detection.

To this end, we present CHOMP (Chewing Side Observation via Multimodal EarPhones), the first system for chewing side detection using earphones. We employ OpenEarable 2.0 [67], a TWS earable research platform that integrates multiple sensing modalities within an earphone form factor, including inner and outer air-conduction microphones, a bone-conduction microphone, an inertial measurement unit (IMU), photoplethysmography (PPG), and a pressure sensor. While each of these modalities has previously been shown to be informative for chewing detection [29, 69], their contributions to classifying the chewing side remain largely unexplored and are therefore systematically evaluated in this work. Furthermore, motivated by prior findings that multimodal sensor fusion can yield complementary and incremental benefits for chewing analysis [46, 58], we examine how combinations of these modalities contribute to CSP assessment.

To evaluate the feasibility of our proposed system, we collected data from 20 participants performing non-chewing activities as well as left- and right-sided chewing across ten food items with varying properties and a full meal. Building CHOMP required overcoming the lack of precise bilateral synchronization in TWS earphones, which necessitated aligning signals across the two devices, as well as fusing heterogeneous, asynchronously sampled signals from multiple sensing modalities. This was achieved by applying the Continuous Wavelet Transform (CWT) to the sensing modalities from both earphones and using the resulting multi-channel scalograms as inputs to CNN-based classifiers with

feature-level fusion. Performance was evaluated using leave-one-food-out (LOFO) and leave-one-subject-out (LOSO) cross-validation (CV) protocols. Our results show that microphones provide the strongest single-sensor unit performance, while fusion with the bone-conduction microphone and IMU further improves detection and maintains robustness under audio interference. These results demonstrate that CHOMP effectively integrates multiple asynchronous modalities in TWS earphones, achieving both high classification performance and practical feasibility for real-world deployment.

Taken together, our key contributions are as follows: (1) we present CHOMP, the first system for chewing side detection using earphones; (2) we collected data from 20 participants across five sensing modalities (microphones, bone-conduction microphone, IMU, PPG, pressure sensor) and show that microphones provide the strongest single-sensor unit performance (LOFO: median $F_1 = 94.5\%$, LOSO: median $F_1 = 92.6\%$) and that fusion with bone-conduction microphone and IMU further elevates performance (LOFO: median $F_1 = 97.7\%$, LOSO: median $F_1 = 95.4\%$); and (3) we demonstrate the robustness of our system under full-meal conditions and three audio noise scenarios.

2 Related Work

In the following, we first introduce the phenomenon of chewing side preference (CSP) and its relation to temporomandibular disorders (TMDs) in Section 2.1 and then review prior wearable-based approaches for detecting the chewing side and TMDs in Section 2.2. Furthermore, we show how previous efforts on chewing detection with earables inform this work in Section 2.3.

2.1 Chewing Side Preference and Temporomandibular Disorders

Chewing side preference is highly prevalent across populations [8, 49, 68] and can already be observed in children [50]. Despite its ubiquity, individuals are often unaware of their tendency [84] and its potential adverse effects. Beyond contributing to asymmetric tooth wear [8], long-term CSP has been associated with morphological alterations in craniofacial structures [33], nasal airway asymmetry [62], and even an increased likelihood of hearing loss [41].

CSP is both a risk factor [8, 84] for developing temporomandibular disorders (TMDs) and a behavioral manifestation in patients with existing TMDs [47, 89]. Over thirty specific TMDs have been identified to date [54], encompassing diverse physiological symptoms, such as joint pain, clicking, and limited motion [48], but also psychological correlates, including depression, anxiety, and sleep disturbances [59]. While up to 40 percent of patients will experience spontaneous resolution of their symptoms [76], high chronic pain is experienced at a nearly quadrupled rate (27 percent) compared to non-TMD patients [54]. The relevance of TMD is further amplified by the fact that temporomandibular joints (TMJ) are among the most frequently used joints in the body, performing opening and closing motions approximately 2,000 times daily [54].

Standardized criteria for the diagnosis of TMD have existed since 1992 [21] and, following a decade-long international validation effort, were updated in 2014 as the *Diagnostic Criteria for Temporomandibular Disorders (DC/TMD)* [75], which are considered current the gold standard for both research and clinical applications. In practice, however, these criteria are rarely applied consistently; practitioners report difficulty in accurate diagnosis [54], and the methods are deemed impractical in routine clinical settings [79]. Furthermore, the current clinical standards rely almost exclusively on self-reports or clinical examinations [20, 54], although imaging techniques are starting to play a role for the diagnosis of TMD [81]. All of these approaches however lack naturalistic behavioral insights and the detection of changes over time. Consequently, objective and longitudinal monitoring of jaw function is rarely performed, prompting calls for the development of innovative approaches [54].

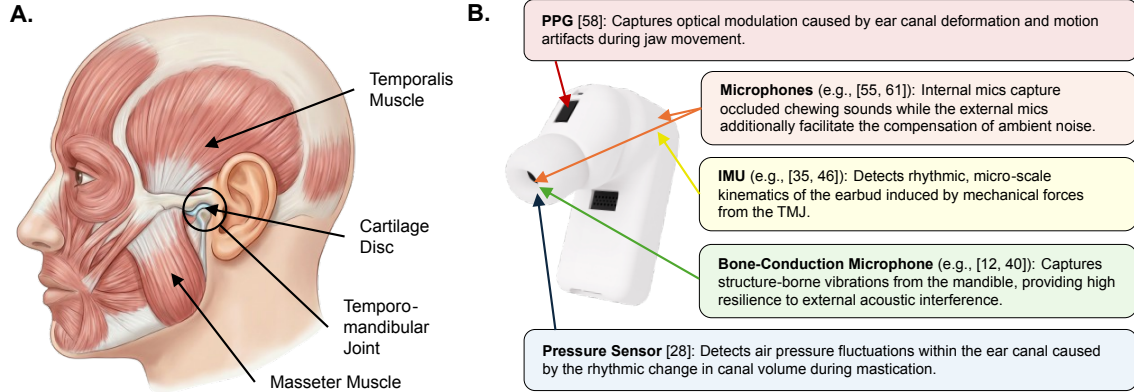


Fig. 2. A. The anatomical structures relevant to TMD are located in close proximity to the ear (adapted from [57]); B. Sensing modalities integrated in OpenEarable 2.0 and their rationale for effective chewing side detection, along with supporting literature on earphone-based chewing recognition.

A wearable solution for monitoring CSP could address these limitations by enabling continuous, naturalistic, and quantitative data collection in everyday life. Such a system would reduce reliance on expert clinical assessments while further offering additional behavioral insights into the condition. It could both identify individuals at elevated risk for developing TMD and track symptom progression in patients already diagnosed, thus supporting earlier interventions and more personalized management.

2.2 Detecting CSP and TMD using Wearable Approaches

To overcome the shortcomings of conventional clinical assessments, several wearable systems have been proposed to capture chewing behavior in everyday settings. For direct TMD diagnosis, Tsuji et al. [85] employed earphones to measure maximum mouth opening and discriminate TMD patients from healthy controls with an AUC of 70.0%. All other wearable approaches focused on identifying CSP, often with regard to TMD [37, 87, 88] and are comprehensively presented in Table 1. Yamasaki et al. [88] presented the first wearable approach by leveraging EMG signals from surface electrodes placed at the left and right masseter muscles. Thereby, they were able to differentiate left and right chewing for two of three tested foods based on contraction amplitudes. Microphone-based approaches have been employed in a series of works by Nakamura et al. [51, 52, 53] using Mel-Frequency Cepstral Coefficients (MFCCs) and cross-correlation features. Placing an array of up to five microphones at the neck, throat, and in front of the mouth led to F_1 performance of up to 81.0% on a left, right, front chewing, and swallowing classification. Conceptually related, Kim et al. [37] describe preliminary work on chewing side detection using an in-ear microphone. The evaluation was restricted to a single participant chewing almonds, with an achieved accuracy of 96.0%. Motion-based approaches leveraged chewing-related movements of the temporalis muscle. Wang et al. [87] used a headband with bilateral IMUs and employed personalized models, thereby achieving 84.8% accuracy in five-fold CV and 81.4% in a leave-one-food-out CV. An approach employing a glasses-type wearable has been presented by Chung et al. [15], who used load cells embedded in the hinges to measure temporalis muscle activity through amplified hinge forces to discriminate left and right chewing within six facial activities in total. Using an SVM with statistical, temporal, and spectral features, the authors achieved F_1 -scores of 89.5% for left and right chewing in a leave-one-participant-out evaluation.

Table 1. Overview of experimental configurations in previous chewing side detection studies in comparison with this work.

Study	Embodiment	Sensor Units Employed	Wireless	Foods	Meal	Audio Robust.
Yamasaki et al. [88]	Surface Electrodes	EMG	No	3	No	No
Nakamura et al. [51]	Neck Clip	Microphones	No	3	No	No
Nakamura et al. [52]	Neck Clip	Microphones	No	5	No	No
Nakamura et al. [53]	Neck Clip, Head Clips	Laryngophones, Microphone	No	5	No	No
Kim et al. [37]	In-Ear Insertion	Microphone	NA	1	No	No
Wang et al. [87]	Headband	IMUs	Yes	8	No	No
Chung et al. [15]	Glasses	Load Cells on Hinges	No	3	No	No
CHOMP	Earphones	Microphones, Bone-Conduction Microphone, IMU, PPG, Pressure Sensor	Yes	11	Yes	Yes

Despite these efforts, existing systems face several limitations. First, except for the glasses in Chung et al. [15], wearables are not naturally integrated into everyday use. Second, robustness remains insufficiently validated, as, with the exception of Wang et al. [87], all studies rely on a narrow set of no more than five foods, and none is demonstrating performance under complex meal conditions or environmental noise. Third, all systems but in Wang et al. [87] rely on tethered or jointly mounted sensing, either via a single bilateral device or wired connections to a separate module. This design enables almost perfect temporal alignment, which is essential for cross-correlational features. In TWS earphones, such precision is unattainable. Considering the mean 2nd intermolar distance of 41 mm [66], the physical time-of-flight (ToF) for acoustic signals is around 12 μ s. Crucially, this physical delay is less than half of the 25 μ s synchronization offset targeted by the Bluetooth LE Audio standard [31]. Consequently, in wireless architectures, the network-induced jitter dominates the physical signal delay, potentially decorrelating high-frequency features that tethered systems capture reliably.

2.3 Chewing Detection with Earables

Although detecting the chewing side has not yet been explored with earphones, a substantial body of work has investigated chewing detection more broadly using earable devices [11, 26, 69, 86]. Most studies focus on identifying chewing episodes and distinguishing them from competing activities, for example speaking or watching movies (e.g., [9, 35, 46]). Some extend this objective by also addressing related tasks, including chew counting [35] or estimating food intake [14], while others concentrate on more specific scenarios, for instance snacking behavior [13] or food-type analysis [5]. Across this literature, approaches primarily rely on either microphones (e.g., [55, 61]) or IMUs (e.g., [35, 46]). A smaller number of works explore alternative sensing strategies comprising bone-conduction microphones [12, 40, 78], proximity sensing [9, 10, 83], PPG [58], or pressure-based sensing [28]. It has further been demonstrated that combining sensing modalities can improve detection performance [46, 58]. Since these approaches often rely on technically demanding configurations or non-standard sensor placements, many systems are built on custom hardware. This heterogeneity in setups and device configurations has produced an equally diverse range of feature-extraction strategies. Prior work employs statistical (e.g., mean, variance, energy [12, 46]), temporal (e.g., zero-crossing rate [28]), kinematic (e.g., jerk [14]) and frequency-based features. Notably, the latter are most consistently employed, especially in the form of MFCCs (e.g., [40, 46, 55]), and have proven effective across multiple systems, thus highlighting their importance for capturing the acoustic and biomechanical signatures of chewing.

Taken together, the literature on chewing detection with earables provides two key insights for our system. First, prior work shows that sensors beyond microphones and IMUs can offer complementary information. Therefore, we

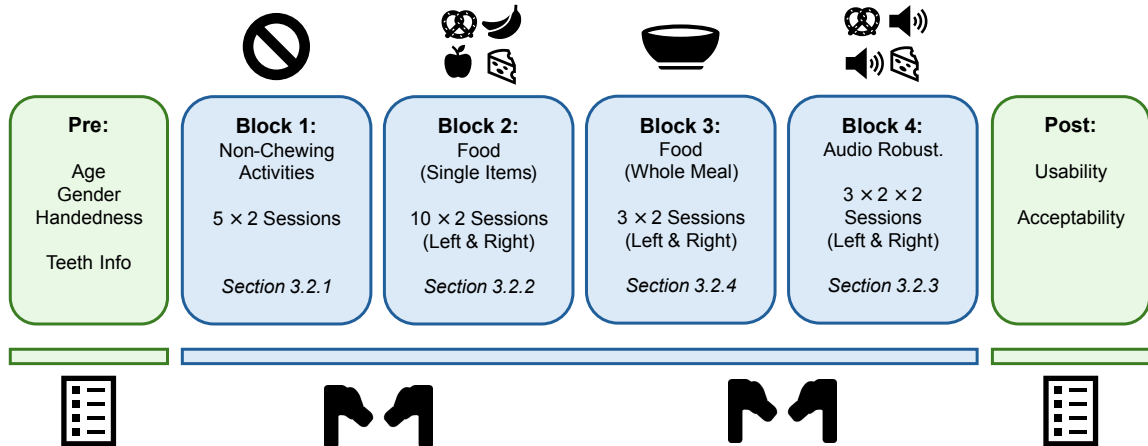


Fig. 3. Experimental overview. Participants completed a pre-questionnaire (see [Appendix A](#)), performed four experimental blocks while wearing OpenEarable 2.0 devices, and then filled out a post-questionnaire (see [Appendix B](#)). Block 1 included five non-chewing activities (see [Section 3.2.1](#)) while Blocks 2–4 comprised different chewing tasks on the left and right side: consumption of ten single food items (see [Section 3.2.2](#)), a whole meal (see [Section 3.2.3](#)), and two selected foods under three audio noise conditions (see [Section 3.2.4](#)).

employ OpenEarable 2.0, which integrates all previously explored sensing modalities except proximity sensing, enabling a systematic evaluation of their contributions to chewing side detection. Second, features such as cross-correlation rely on synchronized information from both sides and, while employed in current wearable research solutions, are hardly feasible within TWS earphones. Consequently, the consistent success of frequency-domain features in prior chewing-detection systems motivates our focus on spectral metrics for chewing side detection.

3 Methodology

In the following, we outline the experimental methodology. First, we describe the employed measurement device, OpenEarable 2.0 [67], and its integrated sensors in [Section 3.1](#). Subsequently, we present the experimental protocol used for the data collection in [Section 3.2](#), including a detailed account of each experimental block and the corresponding design rationale.

3.1 OpenEarable 2.0

Participants wore two OpenEarable 2.0 devices, one on each ear, throughout all recordings. We used the multimodal sensing capabilities of the devices to capture the full range of participants' chewing behavior. Specifically, we employed the 9-axis inertial measurement unit (IMU, 100 Hz), which integrates a 3-axis accelerometer, a 3-axis gyroscope, and a 3-axis magnetometer, although the latter was not used in this study. Furthermore, data were collected from the barometer (100 Hz), the photoplethysmography (PPG) sensor (50 Hz), the 3-axis bone-conduction microphone (1.6 kHz), and both the inner and outer microphones (each 8 kHz). To ensure stable placement in the ear, the devices were fixed with wingtips. An illustration of OpenEarable 2.0 is provided in [Figure 2](#).

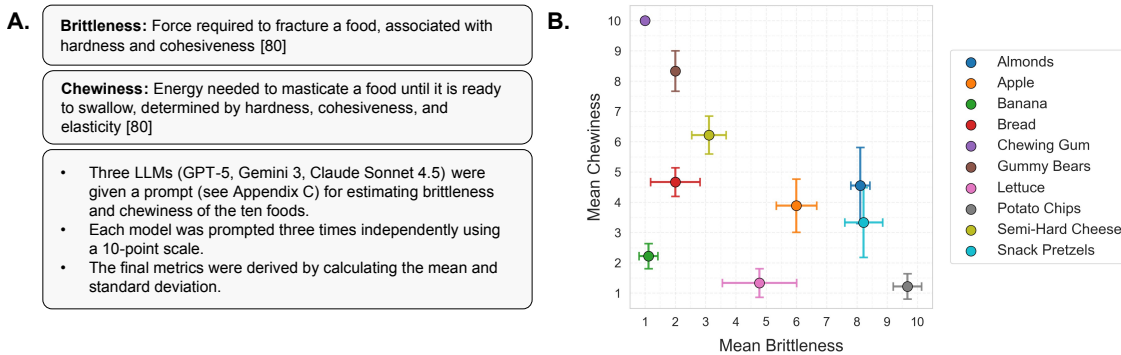


Fig. 4. A. Definitions and procedure of determining brittleness and chewiness; B. Brittleness and chewiness of the selected foods. Nodes depict the means while the whiskers represent standard deviations.

3.2 Experimental Protocol

The experimental protocol consisted of four blocks, complemented by a pre-questionnaire and a post-questionnaire. A schematic overview is provided in Figure 3. The pre-questionnaire collected demographic information (age, gender, handedness) as well as relevant dental details (see Appendix A). Following the data collection, the post-questionnaire assessed participants’ comfort and acceptability of having their chewing behavior recorded with OpenEarables (see Appendix B).

Throughout all experimental blocks, participants wore OpenEarable 2.0 devices to record their behavior. Each block comprised multiple sessions, where one session corresponded to a single 30-second recording. Within each block, sessions were randomized to minimize order effects. All procedures were approved by the university’s ethics committee. The design rationale and structure of each block are detailed in the following.

3.2.1 Non-Chewing Activities. To establish a baseline for distinguishing chewing from non-chewing behavior, we included a set of activities that could be mistaken for chewing. Candidate activities were identified through a literature review, which revealed several commonly applied conditions. Based on prior work, we adopted *sitting still* [22, 23, 35, 46] and *drinking and swallowing* [24, 35, 44, 46], although the latter did not always last the entire 30 seconds of a session. From Ketmalasiri et al. [35], we adapted *head movements*, generalized from side-to-side motion to movements in multiple directions. Their use of emotional facial expressions (happy, sad, angry) was generalized into a task of *drawing faces*. Finally, participants were asked to *read aloud*, reflecting prior use of reading and speaking tasks [22–24, 35, 44, 46]. We did not include *walking* [22, 23], since the study focused exclusively on seated eating (see Section 6.3), nor did we include *watching a movie*, as this aspect was considered addressed in our audio robustness considerations (see Section 3.2.4). In total, five distinct non-chewing activities were selected. For each activity, two sessions were recorded, ensuring balance with the number of recordings from the other conditions.

3.2.2 Food (Single Items). Similar to the selection of non-chewing activities, our choice of foods was guided by prior work in the literature. In addition, we considered key textural characteristics of foods to ensure a representative sample set. According to Szczesniak [80], food texture can be primarily described by mechanical and geometrical properties. Mechanical characteristics capture a food’s response to stress, measured organoleptically through pressures on the teeth, tongue, and palate. For solid foods that require mastication, these characteristics can be reduced to two key

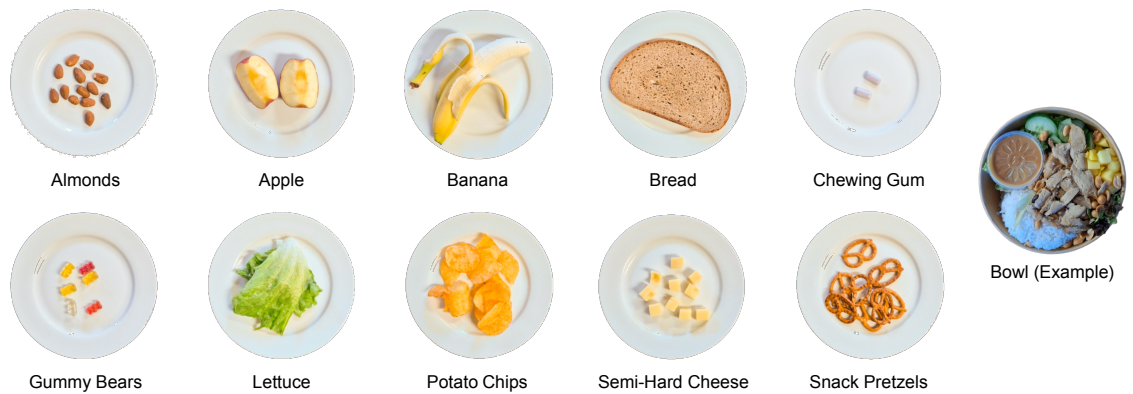


Fig. 5. Selection of different single food items (left) and an example of a whole meal (right).

parameters: First, *Brittleness* is the force required to fracture a food, associated with hardness and cohesiveness. Brittle foods typically exhibit low cohesiveness, variable hardness, and often produce sound during chewing. Second, *Chewiness* describes the energy needed to masticate a food until it is ready to swallow, determined by hardness, cohesiveness, and elasticity. Texture Profile Analysis (TPA) [77] is a standard laboratory method for quantifying these properties via double-compression tests that mimic chewing. However, due to the absence of standardized databases [25] and the requirement of specialized instrumentation, such measurements were not feasible in our study. Instead, we employed three large language models (GPT-5, Gemini 3, and Claude Sonnet 4.5) to estimate the brittleness and chewiness of candidate foods on a 10-point scale, based on the terms' definitions above. Each model was prompted three times independently (with no memory active), yielding nine ratings per food item. We then computed the mean and standard deviation across all ratings. The exact prompting strategy is documented in Appendix C, and the aggregated results are shown in Figure 4. This process resulted in a final selection of ten foods: *almonds* [83, 87], *snack pretzels* [35, 46, 87], *potato chips* [5, 13, 14, 24, 35, 36, 46, 55, 61, 65], *apple* [5, 24, 35, 36, 45, 52, 61, 65, 73], *gummy bears* [87], *chewing gum* [51], *banana* [36, 46, 55], *lettuce* [5, 46, 55], *bread* [5, 24, 35, 45, 73, 87], and *semi-hard cheese* [14].

To provide further balance, half of the selected items are typically consumed by biting into larger pieces (e.g., apple, bread), while the other half are already small enough to be consumed in single portions (e.g., almonds, snack pretzels). This ensured diversity in texture while maintaining comparability across conditions. A photographic overview of all selected foods as used in the experiment is provided in Figure 5. As each food was consumed on each side, this resulted in a total of 20 sessions.

3.2.3 Food (Whole Meal). To approximate a naturalistic eating scenario, participants were provided with a complete meal in addition to individual foods. As with the selection of single food items, care was taken to ensure the meal included a diverse range of consistencies while remaining easy to prepare and acceptable for all participants, including those with individual food preferences. For this purpose, we selected a customizable bowl. Participants were able to choose items from each category, resulting in a meal comprising salad, rice, a crunchy element, a hard and a soft vegetable, and a protein. Detailed specifications of the meal and available options are provided in Appendix D. For each side, three recordings were taken, resulting in six sessions overall.

3.2.4 Audio Robustness. To assess the robustness of the algorithms under noisy conditions, we introduced external disturbances during eating tasks. As repeating all ten food items would have imposed an excessive burden on participants, we selected two representative foods from the set: semi-hard cheese and snack pretzels. These items were chosen because they capture complementary combinations of brittleness and chewiness, making them suitable proxies for the broader food set. Three noise scenarios were applied to simulate realistic or challenging conditions. First, pop chart music was played over the participants’ headphones, reflecting typical listening contexts. Second, dining hall ambiance (mean sound level: 61.8 dB) was played through an external speaker positioned in front of the participant to mimic realistic social eating environments¹. Third, construction noise (mean sound level: 71.3 dB) was presented through an external speaker to replicate high-intensity disturbances that could interfere with the signals². For each noise condition, both selected foods were consumed on each side, resulting in a total of 12 sessions.

3.2.5 Additional Procedures. To control for potential placement effects, participants were asked to remove and reattach the OpenEarable 2.0 devices between ten percent of the sessions. These interventions were distributed to varying points throughout the experiment, thus following no fixed order. Additionally, the experimenter recorded when participants paused to acquire a new piece of food or swallowed on an accompanying smartphone.

4 Model Pipeline

We introduce the CHOMP model pipeline, describing details on sensor data preprocessing in [Section 4.1](#) before presenting the transformation to a suitable input representation in [Section 4.2](#). We furthermore outline the CHOMP model architecture and training procedures in [Section 4.3](#).

4.1 Preprocessing

Timestamps. As discussed in [Section 2.2](#), perfect synchronization of TWS earphones is not feasible. Nevertheless, timestamps of the left and right earables must be aligned to enable joint signal processing. Since firmware version 2.2.2, OpenEarable 2.0 supports global timestamps, which removes the need for manual alignment. At the time of this study, however, firmware version 2.1.5 was the most recent release and did not provide this feature. Manual synchronization was therefore required. Each earable initializes its clock at power-on, creating an initial offset. To estimate this offset for each power cycle, an alignment signal of four Dirac impulses spaced one second apart, followed by four seconds of white noise, was recorded on both earables. Generalized Cross-Correlation with Phase Transform (GCC-PHAT) [39], with phase-only weighting, sharpened the correlation peak, which was smoothed with a Gaussian filter. The temporal offset, determined as the *argmax* of the filtered correlation, was used to align the earables’ clocks. Clock drift was negligible and required no correction. Following alignment, all sensor channels of a common sensor unit were resampled to their target sampling frequency to enforce equidistant timestamps, compensating for slight temporal irregularities. For smartphone annotations (see [Section 3.2.5](#)), each earable streamed optical temperature data at 8 Hz to the smartphone to generate paired timestamps, compensating for the absence of global timestamps.

Filtering. To isolate frequency components related to chewing dynamics while attenuating environmental noise and motion artifacts, we applied a fourth-order Butterworth bandpass filter to all sensor channels. The cutoff frequencies were adapted to each sensor modality. For motion and physiological sensors (IMU, PPG, and pressure sensor), a passband of 0.1 – 6.0 Hz was used. This range captures the fundamental mastication rhythm, which typically lies below 3 Hz,

¹[Dining Hall Ambiance Video](#)

²[Construction Noise Video](#)

while retaining its immediate harmonics and being consistent with prior work [14, 28, 35]. For acoustic and vibration modalities, the bandwidth was extended to capture the spectral characteristics of food comminution and bone-conducted vibrations. The bone-conduction signal was filtered with a passband of 0.1 – 800 Hz, enabling simultaneous analysis of low-frequency jaw motion and higher-frequency structural vibrations, comparable to previous work for noise reduction in contact microphones [36]. Finally, the microphones were filtered with a passband of 0.1 – 4000 Hz to preserve the full acoustic spectrum.

Windowing. Following common practice in sensor-based HAR, we segmented the continuous sensor signals into fixed-length windows. The choice of window size is domain-specific and, for chewing side detection, must reflect the temporal and spectral characteristics of mastication. Prior work has employed window lengths ranging from 1 s [13, 28] to 3 s [14, 15, 35], where shorter windows provide finer temporal resolution and longer windows increase the likelihood of capturing complete chewing cycles. Dominant chewing frequencies have been reported between 0.94 and 2.17 Hz [64], corresponding to chewing cycle durations of approximately 0.5 – 1 s. To reliably capture chewing dynamics relevant for side detection, each window should contain at least one complete chewing cycle. Under worst-case alignment, this requires a minimum window length of approximately twice the maximum cycle duration. Accordingly, we adopted a window length of 2 s. We additionally applied 50% overlap as a form of data augmentation, thus increasing the effective number of training samples. Each window was labeled according to the subject and activity specified in the experimental protocol. We excluded chewing interruptions caused by swallowing or pauses for acquiring a new piece of food, which were manually annotated by the experimenter. Because the precise temporal boundaries of these events cannot be determined with sufficient accuracy to reliably distinguish them from chewing activity, we defined 1 s occlusion zones around each interruption and discarded windows overlapping these zones to minimize label ambiguity and ensure clean training data. Data representing such events were instead obtained from recording sessions dedicated to non-chewing activities, including drinking and swallowing, head movements, and sitting still (see Section 3.2).

4.2 Input Representation

Instead of using raw time-domain signals directly, transforming data into the time-frequency domain can reveal important signal characteristics [2]. Common time-frequency representations include linear and Mel-scaled spectrograms based on the Short-Time Fourier Transform, the Constant Q-Transform, and scalograms derived from the Continuous Wavelet Transform (CWT) [32, 63]. Scalograms are particularly well-suited for chewing detection because they provide adaptive time-frequency resolution, offering higher temporal precision at high frequencies and higher spectral precision at low frequencies. Spectrograms, by contrast, are constrained by a fixed analysis window, which requires a trade-off between temporal and spectral resolution. This limitation is significant for chewing signals, which exhibit rapid temporal variations and frequency patterns across multiple time scales. Scalograms have been successfully applied for both audio [74] and motion sensors, including IMU-based human activity recognition [1, 42]. In our experiments, scalogram-based inputs combined with a CNN backbone achieved the best performance for chewing side detection across all sensors, and were therefore chosen as input representation.

Continuous Wavelet Transform. The CWT of a signal $x(t)$ is defined as the inner product of the signal with a scaled and shifted version of a mother wavelet ψ . In this work, we employ a Complex Morlet wavelet due to its favorable time-frequency localization properties. The transform is given by:

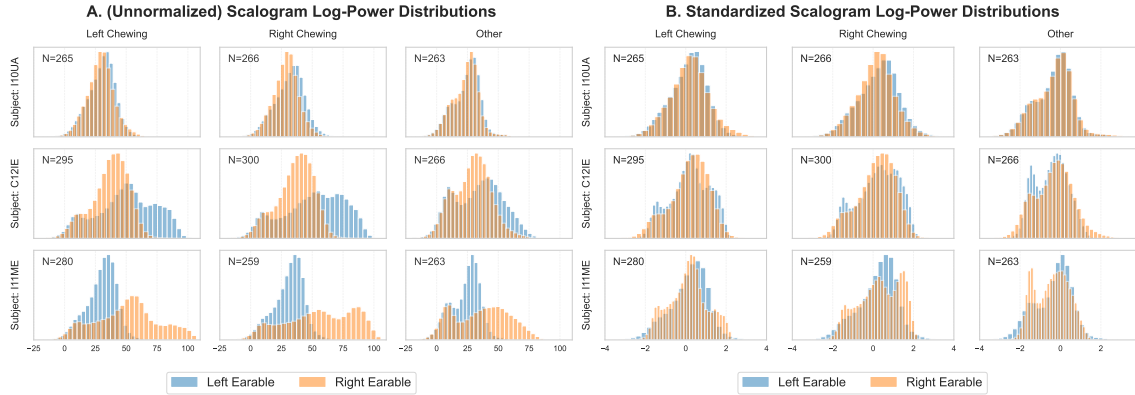


Fig. 6. A. The scalograms across all sensor channels, exemplified here by the inner microphones, reveal inconsistent log-power value distributions between the left and right earables, illustrated here as histograms with sample size N . This discrepancy manifests differently for each subject, suggesting that sensor bias is driven by subject-specific physiology and physical placement rather than just hardware offsets.; B. Applying standardization independently per subject, earable, and sensor channel centers these divergent distributions, enhancing robustness to inter-subject variability.

$$W(s, \tau) = \frac{1}{\sqrt{s}} \int_{-\infty}^{\infty} x(t) \psi^* \left(\frac{t - \tau}{s} \right) dt, \quad \text{where } \psi(t) = \pi^{-1/4} e^{i\omega_0 t} e^{-t^2/2}. \quad (1)$$

Here, s denotes the scale, τ the translation, and $\omega_0 = 6.0$ the central frequency of the Morlet wavelet. To obtain a constant-Q representation, scales s were derived from center frequencies f that were logarithmically spaced between f_{\min} and f_{\max} . This results in higher frequency resolution at lower frequencies and higher temporal resolution at higher frequencies, which is well suited for chewing side detection. Chewing signals comprise low-frequency motion components related to jaw movements as well as higher-frequency acoustic components that occur over shorter time scales. The scale–frequency relationship is defined as:

$$s = \frac{f_s \cdot \omega_0}{2\pi f}, \quad (2)$$

where f_s denotes the sampling rate of the specific sensor unit. To reduce the dynamic range of the wavelet coefficients and emphasize weaker chewing-related while preserving stronger motion-induced components, the complex CWT coefficients were converted into a log-power representation. This transformation improves the robustness of the learned

Table 2. CWT configuration and resulting multi-channel scalogram shapes for the different sensors using a window length of 2 s. For all sensors, the minimum frequency was fixed to $f_{\min} = 0.5$, while the maximum frequency f_{\max} was set to the respective Nyquist frequency of each sensor unit. For the input shape, C refers to the number of sensor channels, F the number of frequency scales, and T the temporal resolution.

Sensor Unit	Sensor Channels	Sampling Rate	Scales	Hop Length	Input Shape (C, F, T)
Microphones (Inner + Outer)	2	8000 Hz	64	128	(4, 64, 125)
Bone-Conduction Microphone	3	1600 Hz	64	32	(6, 64, 100)
IMU (Acc. + Gyro.)	6	100 Hz	64	4	(12, 64, 50)
Pressure Sensor	1	100 Hz	64	4	(2, 64, 50)
PPG (Red, IR, Green)	3	50 Hz	64	2	(6, 64, 50)

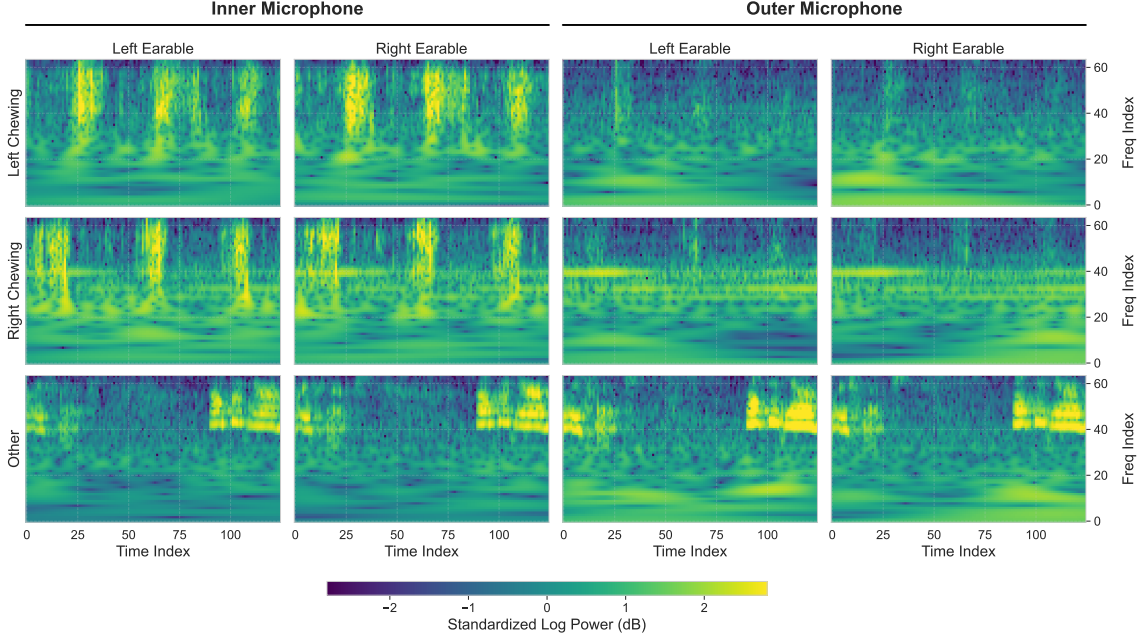


Fig. 7. Comparison of normalized scalograms for inner and outer microphones across both earables. Each row shows a sample from one of the three classes. For *left chewing* and *right chewing*, distinctive vertical pillar-like structures correspond to individual chews and are more pronounced in the inner microphone signals. The *other* class is identifiable by the absence of these periodic patterns. The visual similarity between both chewing classes suggests a model must learn subtle frequency-dependent differences to achieve high classification performance.

features and facilitates the discrimination of side-specific chewing patterns. To avoid numerical issues arising from zero-valued entries, the power values are clamped to a small positive constant ϵ . The resulting log-power scalogram for a given sensor channel is defined as:

$$X = 10 \cdot \log_{10} \left(\max(|W(s, \tau)|^2, \epsilon) \right). \quad (3)$$

Normalization. Analysis of the log-power scalograms, as shown for the inner microphones in Figure 6, reveals inconsistent value distributions between the left and right earables across all subjects and classes. These discrepancies vary by individual, which indicates that sensor bias stems from subject-specific physiology and wearing styles rather than simple hardware offsets. Additionally, different sensor channels exhibit unique value ranges and varying levels of mismatch. Therefore, to address these variations and maintain numerical stability, we apply standardization independently for each subject s , earable e , and sensor channel c according to:

$$\hat{X}_{s,e,c} = \frac{X_{s,e,c} - \mu_{s,e,c}}{\sigma_{s,e,c}}. \quad (4)$$

To prevent data leakage, standardization is carried out separately for the training and test sets, ensuring no test-time information influences the training phase. For each subject, standardization statistics are computed using only that subject's own data. In practice, the system is intended to record chewing activity over a complete eating episode and

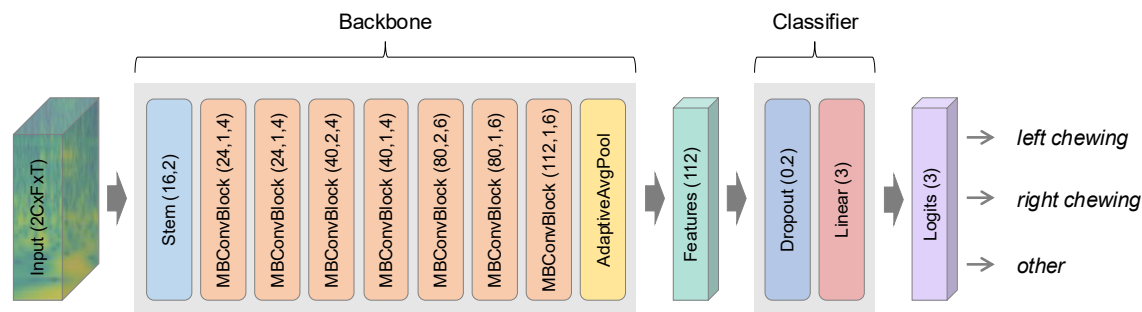


Fig. 8. Overview of the model architecture for the single-sensor configuration based on EfficientNet [82]. The backbone starts with a stem block performing initial spatial downsampling using a stride-2 convolution with 16 output channels, followed by seven efficient MBConv [71] blocks. For each MBConv block, the first parameter specifies the number of output channels, the second the stride, and the third the expansion ratio. The backbone terminates with adaptive average pooling, yielding a feature representation that is fed into a classifier composed of a dropout layer with a rate of $p = 0.2$ and a linear layer projecting the features to logits corresponding to the three classes.

subsequently process these recordings for chewing side analysis, rather than operating in a strictly online, sample-by-sample manner. This usage allows the standardization statistics for an unseen subject to be computed from the recorded data prior to inference. As a result, subject-specific normalization can be applied in deployment, enabling the model to account for individual differences in device placement and anatomy without requiring prior exposure to the subject.

Multi-Channel Scalograms. To capture differences between left- and right-side chewing, signals from both left and right earables were combined, as the use of bilateral data has been shown to improve performance [87]. The scalograms from all sensor channels and both earables were stacked to form a single multi-channel input, producing a 4D tensor $X \in \mathbb{R}^{B \times 2C \times F \times T}$, where B is the batch size, C the number of sensor channels, F the number of frequency scales, and T the temporal resolution. This setup allows a model to learn interactions across both earables and sensor channels.

4.3 Model Architecture

We next present the CHOMP model architecture for chewing side detection from multi-channel scalograms. We begin by describing the feature-extraction backbone, followed by the single-sensor configuration shown in Figure 8 and the sensor-fusion configuration shown in Figure 9. Finally, we describe the model training procedure. All components were implemented using the PyTorch [60] deep learning framework.

Backbone. To capture cross-sensor and cross-earable patterns of chewing activity from the multi-channel scalogram input, we employ a convolutional neural network (CNN) as a backbone. With both performance and computational efficiency in mind, we designed a lightweight architecture based on EfficientNet [82]. While the standard EfficientNet-B0 variant was originally developed to enable efficient on-device inference on resource-constrained platforms such as smartphones, our implementation is tailored to be significantly smaller and more computationally efficient than even this smallest standard variant. This heightened efficiency is achieved by truncating the network depth and capping the maximum channel width of the backbone. The backbone is built around the Mobile Inverted Residual Bottleneck (MBConv) block [71], which exploits depthwise separable convolutions to substantially reduce computational cost compared to standard convolutional layers. The network begins with a stem block consisting of a stride-2 convolution followed by batch normalization and SiLU activation for initial resolution downsampling. This is followed by a sequence

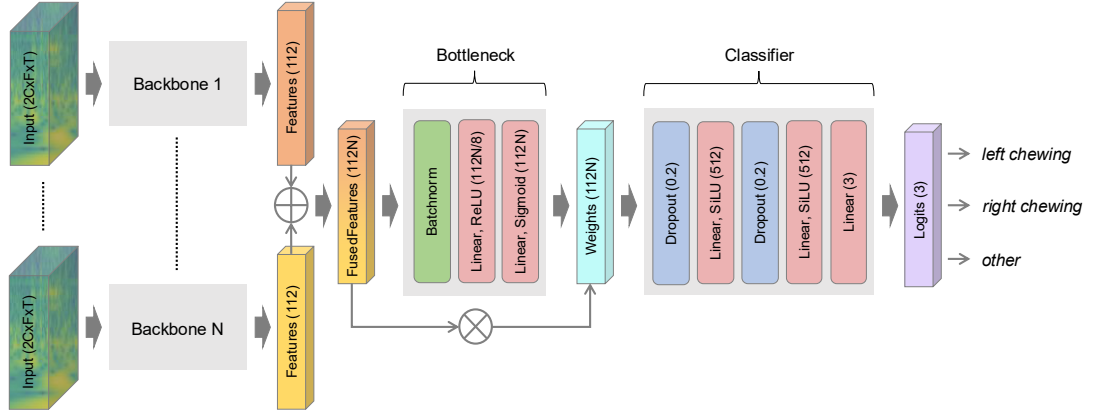


Fig. 9. Overview of the proposed multi-sensor fusion architecture. Independent backbones for N different sensors process sensor-specific scalograms to preserve native resolutions. The resulting features are concatenated, batch-normalized, and passed through an MLP-based gating bottleneck, which generates weighting coefficients for element-wise recalibration of the fused representation. A global MLP-based classification head with SiLU activations and dropout with a rate of $p = 0.2$ then maps these gated features to logits.

of seven MBConv blocks based on an inverted residual design. Within each block, pointwise expansion, depthwise convolution, and Squeeze-and-Excitation modules [30] are employed to dynamically recalibrate feature importance, using SiLU [27] activations throughout. The backbone concludes with a global average pooling layer that produces a 112-dimensional feature representation.

Single-Sensor Configuration. For a single sensor modality, as illustrated in Figure 8, we use a single backbone followed by a lightweight classifier that maps the 112-dimensional feature vector to three logits representing the classes *left chewing*, *right chewing*, and *other*. The *other* class encompasses various types of non-chewing activity, as detailed in Section 3.2.1. This three-class setup is consistent with prior work on chewing-side detection [51]. The classifier is implemented as a single linear layer, motivated by findings from linear probing studies [3], which demonstrate that representations from the final layers of deep networks tend to be highly linearly separable. As a result, a linear classifier is sufficient to attain strong performance, whereas introducing additional fully connected layers would primarily increase the parameter count and the risk of overfitting. For further regularization, a dropout layer with a rate of $p = 0.2$ is applied before the linear layer during training.

Sensor-Fusion Configuration. For sensor fusion, as illustrated in Figure 9, we employ a feature-level late fusion strategy to leverage complementary information from multiple sensor modalities while accommodating their differing input dimensions (see Table 2). Each sensor modality is processed by an independent backbone, producing sensor-specific feature vectors. This modular design preserves the native resolution of each input and avoids aliasing artifacts or information loss associated with early-stage interpolation, while also allowing independent pre-training of the backbones. To combine the modality-specific features, we employ a dynamic gating mechanism inspired by Squeeze-and-Excitation (SE) networks [30]. An MLP-based gating bottleneck computes importance weights based on channel dependencies, which are then applied to recalibrate the concatenated features via element-wise multiplication. While conceptually related to the Gated Multimodal Unit [7], our approach gates the unified feature vector to emphasize multiple complementary

modalities simultaneously, rather than enforcing a strict trade-off. We further depart from Attentional Feature Fusion [17] by replacing complex multi-scale modules with a lightweight MLP to maintain computational efficiency. Finally, the recalibrated features are mapped to logits through a global classification head consisting of linear layers, SiLU activations, and dropout ($p = 0.2$), allowing the model to capture non-linear interactions across sensors while mitigating overfitting.

Training. Both the single-sensor and sensor-fusion configurations were trained using the standard cross-entropy loss and optimized with the Adam optimizer [38]. In the single-sensor configuration, models were trained from scratch with an initial learning rate of 1×10^{-3} . For the sensor-fusion configuration, backbones pretrained in the single-sensor configuration were reused and initially frozen, while the newly introduced global classifier was trained for three epochs as a warm-up phase. Afterward, all parameters were unfrozen and jointly optimized using an initial learning rate of 1×10^{-4} . Pretraining was performed for up to 100 epochs, whereas fusion training was conducted for up to 30 epochs, both with a batch size of 64. A validation split of 20% of the training data was used, together with early stopping with a patience of 20 epochs to mitigate overfitting. Dropout layers were active only during training.

5 Evaluation

In the following, we first describe the final dataset assembled from the conducted experiments in Section 5.1. We then evaluate the performance of CHOMP in both the single-sensor (Section 5.2) and sensor-fusion (Section 5.3) configurations. Performance under audio noise conditions is examined in Section 5.4. Finally, we evaluate edge deployment feasibility in Section 5.5 before assessing the usability and acceptability of utilizing OpenEarable 2.0 for chewing side detection in Section 5.6.

5.1 Dataset

Since one participant was excluded due to corrupted synchronization files, the final dataset comprised 20 subjects (13 male, 7 female). Each participant received a €15 Amazon voucher and the remaining contents of the bowl as compensation. Participants had a mean age of 26.3 years ($SD = 9.3$, range : 20 – 55), and all but three were right-handed. In accordance with the exclusion criterion of having no missing teeth, all included participants had a complete set of permanent teeth, except for wisdom teeth, which were present in only three participants. Tooth restorations were reported by five participants. After preprocessing (see Section 4.1), the resulting dataset comprised 15,806 samples.

5.2 Single-Sensor Evaluation

We begin the evaluation of chewing side detection with the single-sensor unit configurations of the model architecture described in Section 4.3, trained independently for each of the five sensing modalities. To closely approximate real-world deployment conditions, we evaluated subject generalization using a leave-one-subject-out (LOSO) CV protocol. In addition, given the domain-specific relevance for chewing side detection, we examined the model’s ability to generalize to previously unseen food types, therefore additionally conducting a leave-one-food-out (LOFO) CV. Performance is reported using median F_1 scores along with interquartile ranges (IQR) to account for outliers. For comparison, we include a baseline Random Forest (RF) approach that closely follows prior work on chewing detection [35, 46], using time-domain (mean, variance, power) and frequency-domain (spectral centroid, MFCCs) features as inputs. The full specification of the RF baseline is provided in Appendix E.

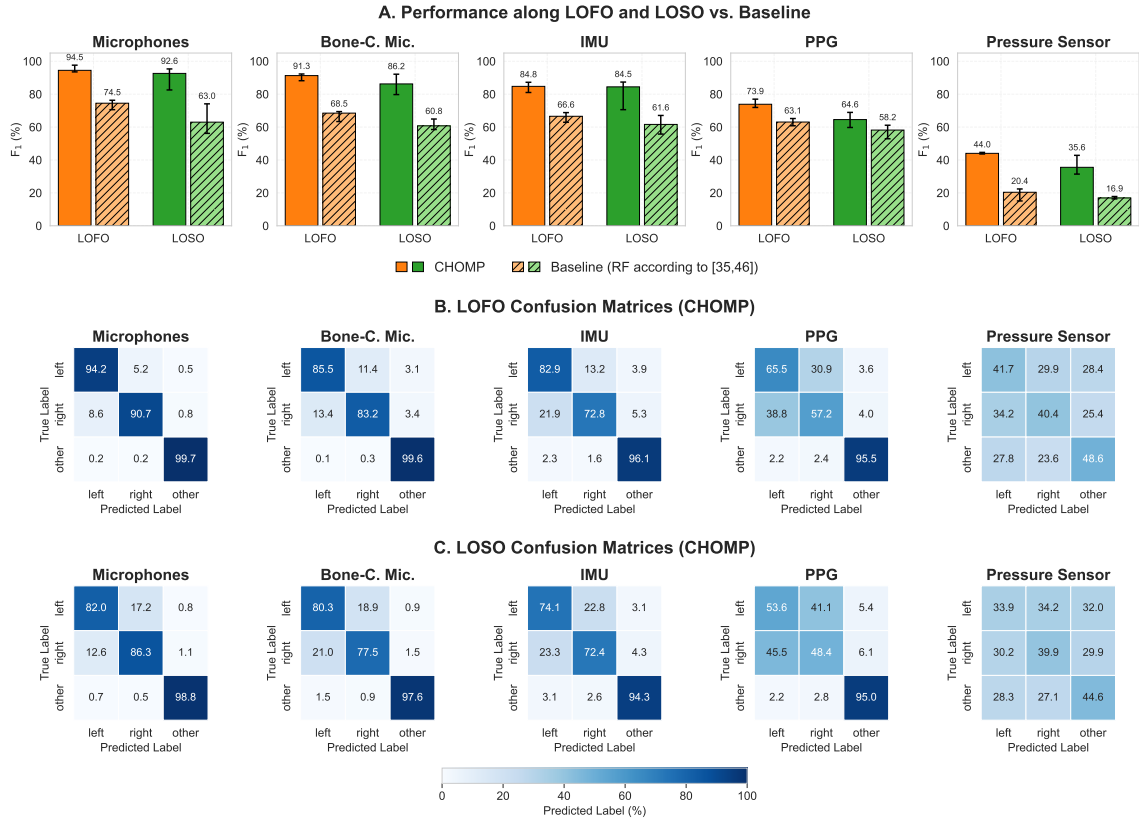


Fig. 10. Single-Sensor Results: A. Classification performance shown as median F_1 scores with interquartile ranges (Q1-Q3) for CHOMP and the baseline Random Forest (RF) approach [35, 46], evaluated along five sensor modalities across LOFO and LOSO CV protocols.; B-D Confusion matrices for CHOMP across LOFO and LOSO.

Results are presented in Table 3 and Figure 10. The microphones achieve the highest performance, with median F_1 scores of 94.5% for LOFO and 92.6% for LOSO. Across the two evaluation protocols, the bone-conduction microphone trails the microphones by 4.8%, and the IMU performs lower by 8.9%. The PPG sensor exhibits noticeably reduced performance, reflecting its limited ability to differentiate left- and right-sided chewing, while the pressure sensor performs near-randomly across all three classes. Notably, all CHOMP models consistently outperform the RF baseline across sensor modalities and evaluation protocols, with largest improvements for the microphones (20.0% under LOFO and 29.6% under LOSO). Moreover, the LOFO performance over all sensor modalities exceeds LOSO by 5.0%, indicating that inter-subject variability has a larger impact on chewing side recognition than variability in food characteristics.

5.3 Sensor-Fusion Evaluation

Next, we evaluated whether fusing sensor modalities could further improve chewing side detection, following the sensor-fusion configuration described in Section 4.3. For this analysis, we focused on the microphones, the bone-conduction microphone, and the IMU, as these modalities had shown the ability to discriminate between chewing sides

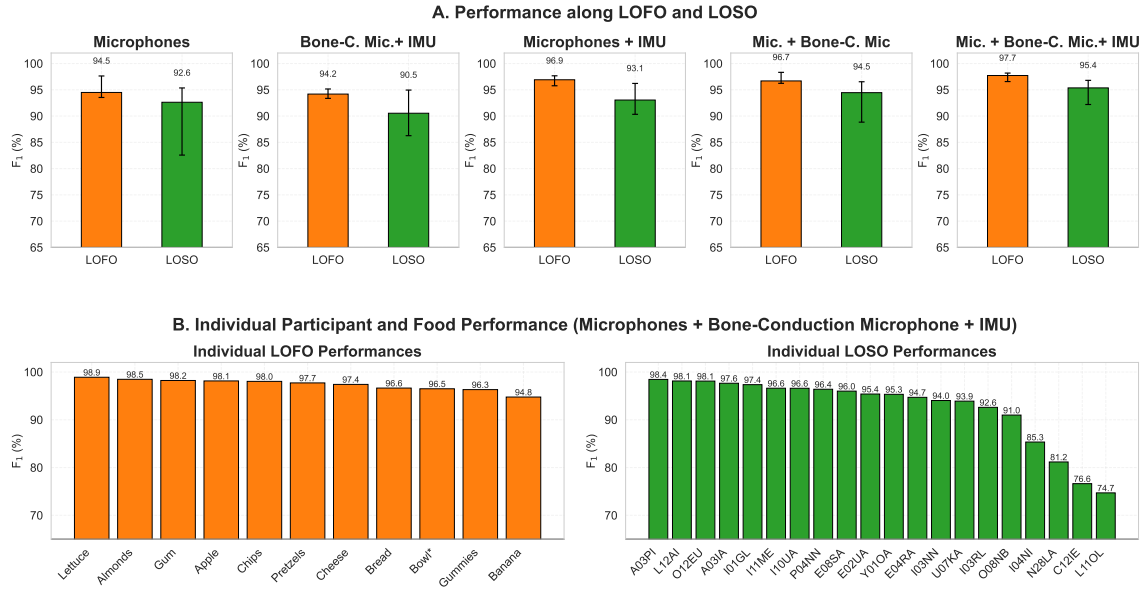


Fig. 11. Sensor-Fusion Results: A. Classification performance shown as median F_1 scores with interquartile ranges (Q1-Q3) for CHOMP along combinations of microphones, bone-conduction microphone, and IMU, evaluated across LOFO and LOSO CV protocols. Performance of microphones is displayed for reference.; B. Performance under LOFO and LOSO CV for individual foods and subjects using sensor-fusion configuration of all three sensor modalities. The (*) indicates results obtained with reduced training data, as bowl runs are three times more frequent than single food trials.

in the single-sensor evaluation. We tested all possible pairs and the full three-sensor combination, resulting in four combinations in total.

Results are detailed in Table 4 and Figure 11. All sensor-fusion configurations, except the bone-conduction microphone-IMU pair, consistently outperformed the microphones-only benchmark. Among two-sensor combinations, microphones and the IMU achieved the highest LOFO performance (96.9%), while microphones and the bone-conduction microphone performed best for LOSO (94.5%). The integration of all three sensor units provided a further performance boost of 0.8 – 0.9%. Examining LOFO performance across foods for the full sensor trio shows that even the lowest-performing banana reached 94.8%, while apple achieved 98.9%. For LOSO, individual performance exceeded 90% for 16 participants, reaching a maximum of 98.4%, although four participants trailed with F_1 scores between 74.7 and 85.3%.

5.4 Audio Robustness Evaluation

To assess robustness under realistic acoustic interference, we leveraged two additional sessions for semi-hard cheese and snack pretzels recorded under the three noise conditions, of which dining hall and construction noise was played through an external speaker while music was played directly through the earphones (see Section 3.2.4). We repeated the training and evaluation procedures used for the single-sensor and sensor-fusion configurations, considering each noise condition individually as well as their combination. This setup increased the amount of chewing data by approximately 15% per noise condition (46% when combined), albeit with introduced signal interference.

Results are shown in Table 5 and in Figure 12. Construction noise resulted in the largest performance degradation, with an average reduction in median F_1 scores of 1.5%, followed by music played through the earphones (1.3%) and

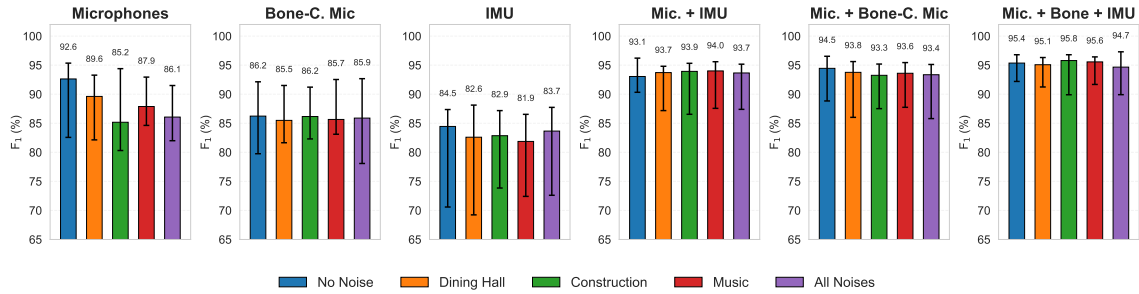


Fig. 12. Audio robustness results shown as median F_1 scores with interquartile ranges (Q1-Q3) for single-sensor configurations of the microphones, the bone-conduction microphone, the IMU, and their combinations including microphones, evaluated under a LOSO CV protocol. For each of the three noise conditions and their combination, four additional sessions (two with semi-hard cheese and two with snack pretzels) were added to the dataset and used for training and evaluation. Performance without added noise is displayed for reference.

dining hall ambiance (1.0%). When all three noise conditions were combined, the median F_1 decreased by 1.5%. An analysis of individual sensing modalities shows that the performance of microphones degrades by 5.4% under noise. The bone-conduction microphone and the IMU are only slightly affected with reductions of 0.4% and 1.7%, respectively. Consistent with this observation, fusion of microphones and IMU shows a slight performance increase (+0.7), while the combination of microphones and bone-conduction microphone exhibits a modest decline of 1.0%. In contrast, fusion of all three modalities remains robust, with a minor decrease of 0.1% and a median F_1 of 95.3%.

5.5 Edge Deployment Feasibility

As described in Section 4.3, the CHOMP model architecture for both single-sensor and sensor-fusion configurations was designed with smartphone deployment as a primary constraint. Table 6 shows that all configurations remain compact, with model sizes from 2.06MB for single-sensor models up to 8.00MB for full sensor fusion, and FLOPs ranging from 26.77M to 126.73M, well within the capabilities of modern mobile CPUs. On-device measurements on a Google Pixel 8a confirm feasibility: single-sample inference latencies stay below 2 ms for individual sensors and under 9 ms for full fusion, with RAM usage under 16MB. For 450-sample windows corresponding to 15 minutes of eating activity, latency and memory scale predictably, but remain practical for on-device processing of complete meal recordings for subsequent chewing side analysis. Single-sensor configurations incur the smallest computational cost, increasing from the IMU to the bone-conduction microphone and microphones, while sensor-fusion models scale with the number of modalities, as each requires its dedicated backbone.

5.6 Usability and Acceptability Analysis

All items evaluating the usability and acceptability of using OpenEarable 2.0 for chewing side detection were answered on a 7-point Likert scale (1 = *Totally Disagree*, 7 = *Totally Agree* or 1 = *Very Uncomfortable*, 7 = *Very Comfortable*, respectively). Overall results are summarized in Figure 13 and the full questionnaires are provided in Appendix B.

Usability. Results indicate that OpenEarable 2.0 devices were generally comfortable to wear ($M = 5.60$) and, on average, fit the ears well ($M = 5.55$). Participants reported little to no pain or irritation ($M = 5.8$). Movements of the earables caused only few distracting noises ($M = 2.35$, inverse item) and did only slightly interfere with eating

Table 3. Single-Sensor Results, reported as median F_1 scores with interquartile ranges (Q1-Q3), along with precision and recall, for CHOMP and the Random Forest (RF) baseline approach [35, 46] across LOFO and LOSO CV protocols.

Sensor Units	CHOMP						Baseline					
	LOFO			LOSO			LOFO			LOSO		
	F_1 (IQR)	Pre.	Rec.									
Microphones	94.5 (93.5-97.6)	94.5	94.5	92.6 (82.6-95.3)	92.8	92.7	74.5 (70.6-76.3)	75.7	74.6	63.0 (56.2-74.1)	77.2	67.9
Bone-Conduction	91.3 (88.2-92.3)	91.5	91.3	86.2 (79.8-92.1)	87.2	86.4	68.5 (63.4-69.4)	69.5	70.0	60.8 (58.5-64.9)	65.9	64.8
IMU	84.8 (81.0-87.2)	85.5	84.5	84.5 (70.6-87.4)	84.9	84.4	66.6 (62.9-68.8)	66.7	67.0	61.6 (55.8-67.1)	63.5	62.7
PPG	73.9 (71.9-77.0)	75.7	75.0	64.6 (59.8-68.9)	66.6	66.0	63.1 (60.8-65.2)	62.9	64.1	58.2 (52.9-61.1)	60.2	59.3
Pressure Sensor	44.0 (43.7-44.6)	46.0	43.8	35.6 (31.4-42.8)	36.2	36.0	20.4 (15.1-22.4)	22.5	32.5	16.9 (16.3-17.8)	11.9	33.3

Table 4. Sensor-Fusion Results, reported as median F_1 scores with interquartile ranges (Q1-Q3), along with precision and recall and across LOFO and LOSO CV protocols.

Sensor Units	LOFO			LOSO		
	F_1 (IQR)	Pre.	Rec.	F_1 (IQR)	Pre.	Rec.
Bone-C. Mic. + IMU	94.2 (93.4-95.2)	94.2	94.2	90.5 (86.3-94.9)	90.7	90.6
Microphones + IMU	96.9 (95.8-97.7)	96.9	96.9	93.1 (90.3-96.2)	93.5	93.1
Microphones + Bone-C. Mic.	96.7 (96.2-98.3)	96.7	96.7	94.5 (88.8-96.5)	94.7	94.5
Microphones + Bone-C. Mic. + IMU	97.7 (96.6-98.2)	97.7	97.7	95.4 (92.2-96.8)	95.4	95.4

Table 5. Audio Robustness Results, reported as median F_1 scores with interquartile ranges (Q1-Q3) along with precision and recall, under a LOSO CV protocol. For each of the three noise conditions and their combination, four additional sessions (two with semi-hard cheese and two with snack pretzels) were added to the dataset and used to train and evaluate noise-specific models.

Sensor Units	Dining Hall			Construction			Earphone Music			All Noises		
	F_1 (IQR)	Pre.	Rec.									
Microphones	89.6 (82.1-93.3)	90.3	89.7	85.2 (80.3-94.4)	87.6	85.4	87.9 (84.6-92.9)	89.9	88.0	86.1 (82.0-91.5)	87.8	86.1
Bone-C. Mic.	85.5 (81.6-91.5)	87.4	85.8	86.2 (82.3-91.2)	87.1	86.3	85.7 (83.1-92.5)	86.0	85.6	85.9 (78.1-92.7)	86.6	86.0
IMU	82.6 (69.2-88.1)	83.7	82.9	82.9 (73.9-87.2)	84.1	82.8	81.9 (72.4-86.5)	84.1	82.1	83.7 (72.6-87.7)	84.6	83.7
Mic. + IMU	93.7 (87.2-94.8)	93.8	93.7	93.9 (86.5-95.3)	94.0	93.9	94.0 (87.6-95.6)	94.3	94.0	93.7 (87.4-95.2)	93.7	93.7
Mic. + Bone	93.8 (86.0-95.6)	94.2	93.8	93.3 (87.5-95.2)	93.4	93.3	93.6 (87.7-95.4)	94.1	93.6	93.4 (85.8-95.1)	93.6	93.4
Mic. + Bone + IMU	95.1 (91.2-96.3)	95.3	95.1	95.8 (89.9-96.8)	96.1	95.8	95.6 (91.7-96.4)	95.6	95.6	94.7 (89.9-97.3)	94.8	94.7

Table 6. Model complexity and computational footprint for different sensor configurations. Metrics include total parameters, model size, and Floating Point Operations (FLOPs). Additionally, inference latency and RAM usage were measured on a Google Pixel 8a using ExecuTorch [60] with the CPU-based XNNPACK backend, representing the average of 10 measurements. Models were captured using Ahead-of-Time compilation without quantization. The 450-sample batch size corresponds to 15 minutes of eating activity, roughly corresponding to a full meal.

Sensor Units	Params (M)	Size (MB)	FLOPs (M)	Latency (ms) (1 / 450 samples)	RAM (MB) (1 / 450 samples)
IMU	0.53	2.06	26.77	1.36 / 869.34	4.01 / 650.93
Bone-Conduction Microphone	0.53	2.06	49.75	1.78 / 1620.75	5.17 / 1046.38
Microphones	0.53	2.06	61.65	1.93 / 2008.71	5.91 / 1177.89
IMU + Bone-C. Mic.	1.45	5.66	76.91	8.08 / 2477.25	10.25 / 1534.15
IMU + Microphones	1.45	5.66	88.81	7.17 / 2817.25	10.60 / 1680.09
Bone-C. Mic. + Microphones	1.45	5.66	111.79	3.83 / 3543.64	11.42 / 1855.60
IMU + Bone-C. Mic. + Microphones	2.05	8.00	126.73	8.39 / 4385.52	15.19 / 2286.95

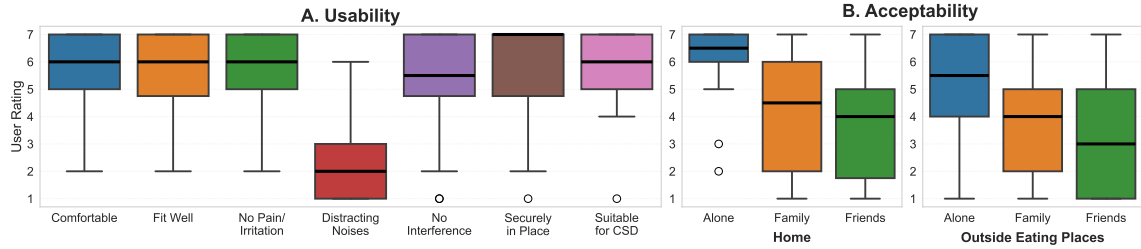


Fig. 13. Usability (A.) and acceptability (B.) analyses. For acceptability, ratings for outside eating places (dining hall, fast-food place, café, and restaurant) are aggregated into a single plot.

($M = 5.15$). Participants predominantly indicated that the earables stayed securely in place while moving or chewing ($M = 5.65$) and considered them suitable for detecting the chewing side ($M = 5.65$).

Acceptability. Participants showed a clear preference for using earables for chewing side detection when eating alone ($M = 5.38$) compared to eating with family ($M = 3.75$) or friends ($M = 3.40$). Moreover, using the earables at home ($M = 4.68$) was preferred over use in public eating environments, including dining halls ($M = 4.30$), fast-food place ($M = 4.12$), cafés ($M = 3.97$), and restaurants ($M = 3.82$). Accordingly, deploying earables for chewing side detection when eating at home alone was most favorable ($M = 6.05$).

6 Discussion

In this work, we introduce CHOMP, the first system for chewing side detection using earphones. We explored the feasibility of employing OpenEarable 2.0 devices and evaluated the contributions of five different sensing modalities, showing that microphones achieve the highest performance (LOFO: 94.5%, LOSO: 92.6%) and that fusing them with the bone-conduction microphone and the IMU further elevates detection (LOFO: 97.7%, LOSO: 95.4%). Additionally, we demonstrated the robustness of our system under three different noise conditions as well as the feasibility of edge deployment and inference. Furthermore, we found that participants’ responses indicated high usability for employing OpenEarable 2.0 for chewing side detection. We next explore our results in further detail (Section 6.1), highlight their real-world applicability and clinical implications (Section 6.2), and identify limitations and future opportunities (Section 6.3).

6.1 Exploration of Results

In the following, we discuss different aspects of our results.

6.1.1 Earphones for Chewing Side Detection. This study is the first to demonstrate the feasibility of employing earphones for chewing side detection. Moreover, we show that this task can be reliably addressed using TWS earphones, now the dominant consumer form factor, which inherently limits cross-correlative features due to network-induced jitter at short temporal scales [31]. Our results demonstrate that such features are not required to achieve high performance. Motivated by the effectiveness of frequency domain representations in chewing detection (see Section 2.3), we applied the CWT to each sensing modality and used the resulting multi-channel scalograms as inputs to CNN-based classifiers. While none of the previous wearable approaches for chewing side detection reported F_1 scores above 90% [15, 53, 87], we outperform this level already using microphones alone. Beyond this, we are the first to demonstrate the substantial

Table 7. Correlations between median F_1 performance scores (across participants and foods) and usability questionnaire items or food characteristics, respectively. Significant correlations are marked with (*). Statistical power is limited due to the small sample size (20 participants, 10 foods) and ceiling effects for the questionnaire items.

Sensor Units	Comfortable	Fit Well	Securely in Place	Brittleness	Chewiness
Microphones	0.26	0.05	0.25	0.52	-0.31
Bone-Conduction Microphone	0.34	0.14	0.42	0.49	-0.35
IMU	0.14	0.05	0.27	0.27	-0.69*
Bone-C. Mic. + IMU	0.24	0.14	0.35	0.69*	-0.47
Mic. + Bone-C. Mic.	0.45*	0.20	0.40	0.56	-0.07
Microphones + IMU	0.29	0.10	0.24	0.58	-0.35
Mic. + Bone-C. Mic. + IMU	0.37	0.19	0.32	0.57	-0.04

benefits (+3.0%) of fusing multiple sensing modalities for chewing side detection, highlighting the complementary nature of heterogeneous sensors that capture different aspects of the chewing process. While microphones, the bone-conduction microphone, and the IMU perform well, the PPG and pressure sensor yield weaker results, despite their reported success in chewing detection [28, 58]. As shown in Section 5.2, PPG primarily distinguishes chewing from non-chewing activities but fails to discriminate the chewing side, whereas pressure sensing generally provides poor performance. These limitations can be partly attributed to prior studies’ use of custom devices, particularly for ear canal pressure sensing [28], which requires a well-sealed ear canal, a condition often ensured in specialized hardware [6, 70], but not reliably met in our setup.

6.1.2 Inter-Subject Variability. More consequential than differences between sensing modalities are inter-subject variations. In Section 5.3, we showed that four participants underperformed compared to the rest. Correlations between F_1 scores and usability questionnaire items presented in Table 7 suggest that earphone fit was a key factor, as all related items were consistently correlated with higher performance throughout sensing modalities. The worst performing subject, for example, was the only one to totally disagree that the earables stayed securely in place. This suggests that the primary limitation was not the detection approach itself but suboptimal earphone fit. Simple mitigations include verifying earphone fit before use [18], while more advanced solutions could involve personalized eartips [90].

6.1.3 Inter-Food Variability. As described in Section 3.2.2, foods were selected to cover a balanced range of brittleness and chewiness. This variation in food texture reduces reliance on food-specific cues and supports the learning of representations that generalize across eating conditions. Analysis of the relationship between model performance and food characteristics validates this choice: brittleness consistently exhibits a positive association with median F_1 performance, with average correlations of $r = 0.43$ for single-sensor configurations and $r = 0.60$ for sensor-fusion configurations. In contrast, chewiness is consistently negatively correlated with performance (single: $r = -0.45$; fusion: $r = -0.23$), indicating that softer, more deformable foods yield less distinctive chewing signatures, thereby increasing classification difficulty. In addition, by incorporating a full meal composed of heterogeneous food components, we extend evaluations beyond isolated food items toward more naturalistic eating scenarios.

6.1.4 Noise Robustness. Complementing this, our audio robustness experiments indicate that chewing side detection performance remains largely stable under common acoustic interferences, including music played through the earphones and typical dining hall ambient noise. Acceptability analysis further reveals that users are most likely to employ CHOMP alone at home, where environmental noise is minimal and models can operate at full capacity. Additionally, sensor

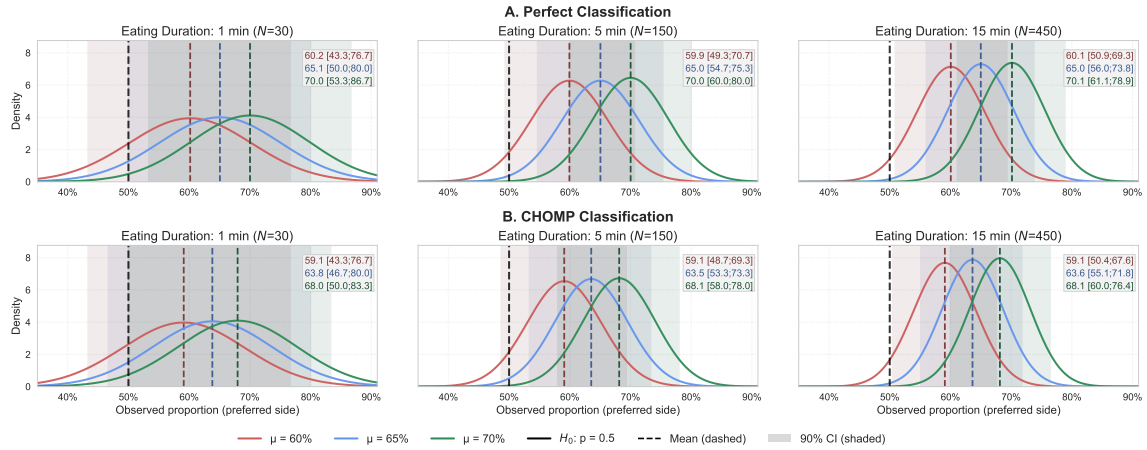


Fig. 14. Distribution of observed chewing side proportions (left/right) under A. perfect classification and B. CHOMP classification (i.e., $LOSO F_1 = 95.4\%$) across eating durations (1, 5, and 15 minutes). Each panel shows three simulated patient types with true chewing side preferences of $\mu \in \{60\%, 65\%, 70\%\}$, modeled as $\mathcal{N}(\mu, 5\%)$ to represent meal-to-meal variability. Distributions are generated via Monte Carlo simulation ($N = 10,000$). Reported values show mean observed proportion and 90% confidence intervals. Under perfect classification (A.), observed distributions match true preferences. Under CHOMP with 4.6% misclassification rate (B.), distributions compress slightly toward 50% (e.g., 1.4 percentage point shift for $\mu = 65\%$). Furthermore, 90% confidence intervals exclude the 50% threshold after: 1 minute for $\mu = 70\%$, 5 minutes for $\mu = 65\%$, and 15 minutes for $\mu = 60\%$, enabling statistically confident CSP diagnosis. The minimal performance degradation from perfect to CHOMP classification demonstrates clinical viability for real-world deployment.; *Note*: For simplicity, the analysis considers binary left/right classification as other activities were rarely classified as chewing (see Section 5.2).

modality evaluations showed that the system was able to almost perfectly discriminate between chewing and non-chewing activities, comprising e.g., talking or head movements (see Section 5.2). Results therefore suggest that the proposed approach is well-suited for everyday deployment under typical eating conditions.

6.2 Real-World Applicability and Clinical Implications

Considering that approximately a third of the global population is affected by TMDs [4, 91], the potential impact of unobtrusive, longitudinal monitoring solutions is immense. As described in Section 2.1, current TMD assessment and diagnosis largely rely on self-reports and clinical examinations [20, 54], providing only limited insight into naturalistic eating behavior and its evolution over time. CHOMP fills this gap, therefore representing one of the innovative approaches called for by practitioners [54]. As CSP is a manifestation of TMDs [47, 89], monitoring the chewing side provides an opportunity to observe jaw functionality while also being easily integrable into existing clinical instruments, such as symptom diaries. Given that a CSP itself can not only contribute to TMDs [8, 84] but has further been associated with other conditions such as alterations in craniofacial structures [34], integrating it into wearable health solutions has high potential impact. Since CHOMP is efficient enough for deployment and inference on edge devices such as smartphones (see Section 5.5), it could be widely accessible, enabling broad adoption, raising awareness, and supporting preventive behaviors. We have demonstrated robustness to noise and evaluated the system across a wide range of foods and participants, indicating that CHOMP is well-equipped for real-world deployment. The practical utility of the system is further illustrated in Figure 14, which shows that CSP can be monitored with minimal bias and that reliable identification of CSP is achievable with only a few minutes of data. Together, these findings suggest that the CHOMP

could realistically complement clinical practice by providing objective, longitudinal insights into everyday chewing behavior, helping clinicians and patients alike.

6.3 Limitations and Future Work

The chosen experimental setup imposes several limitations as participants were restricted in the amount of food they could consume. First, we only studied eating while sitting, as this reflects the most common eating posture. Second, we did not collect data for bilateral chewing, as doing so would have increased data collection effort by half. This choice aligns with prior work on chewing side detection, which also excludes bilateral chewing, reflecting the natural tendency to predominantly chew on one side (Section 2.2). Third, we included only participants without missing teeth (excluding wisdom teeth), which limits external validity for elderly populations or individuals with partial tooth loss. Finally, future work could explore adaptive models such as test-time adaptation [43] to individualize detection to specific chewing styles or food types, thus further improving robustness in real-world deployment.

7 Conclusion

In this paper, we presented CHOMP, the first system for chewing side detection using earphones. Our multimodal sensor fusion approach achieves median F_1 scores of 97.7% in LOFO and 95.4% in LOSO CV, representing the highest classification performance reported to date for chewing side detection by wearable systems, while remaining robust across diverse food types and audio noise conditions. By enabling continuous and unobtrusive monitoring of chewing side in real-world eating environments, CHOMP provides a practical pathway for both clinicians and patients to assess jaw function in daily life. This information can support the diagnosis and longitudinal monitoring of TMDs and enables early detection of emerging chewing side preferences, thereby opening new opportunities for preventive interventions before maladaptive chewing patterns become habitual.

Acknowledgments

Funded by the German Research Foundation (Deutsche Forschungsgemeinschaft – DFG) – GRK2739/1 – Project Nr. 447089431 – Research Training Group: KD²School – Designing Adaptive Systems for Economic Decisions.

References

- [1] Nadeem Ahmed, Md Obaydullah Al Numan, Raihan Kabir, Md Rashedul Islam, and Yutaka Watanobe. 2024. A robust deep feature extraction method for human activity recognition using a wavelet based spectral visualisation technique. *Sensors* 24, 13 (2024), 4343.
- [2] Aydin Akan and Ozlem Karabiber Cura. 2021. Time–frequency signal processing: Today and future. *Digital Signal Processing* 119 (Dec. 2021), 103216. doi:10.1016/j.dsp.2021.103216
- [3] Guillaume Alain and Yoshua Bengio. 2016. Understanding intermediate layers using linear classifier probes. *arXiv preprint arXiv:1610.01644* (2016), 13.
- [4] Ahmed Yaseen Alqutaibi, Maged S. Alhammedi, Hatem Hazzaa Hamadallah, Ammar Abdulrahman Altarjami, Omar Talal Malosh, Aseel Mohammed Aloufi, Lama Mohammed Alkahtani, Faten Safran Alharbi, Esam Halboub, and Abeer A. Almashraqi. 2025. Global prevalence of temporomandibular disorders: a systematic review and meta-analysis. doi:10.22514/jofph.2025.025
- [5] Oliver Amft and Gerhard Troster. 2009. On-Body Sensing Solutions for Automatic Dietary Monitoring. *IEEE Pervasive Computing* 8, 2 (April 2009), 62–70. doi:10.1109/MPRV.2009.32
- [6] Toshiyuki Ando, Yuki Kubo, Buntarou Shizuki, and Shin Takahashi. 2017. CanalSense: Face-Related Movement Recognition System based on Sensing Air Pressure in Ear Canals. In *Proceedings of the 30th Annual ACM Symposium on User Interface Software and Technology (UIST '17)*. Association for Computing Machinery, New York, NY, USA, 679–689. doi:10.1145/3126594.3126649
- [7] John Arevalo, Tamar Solorio, Manuel Montes-y Gómez, and Fabio A González. 2017. Gated multimodal units for information fusion. *arXiv preprint arXiv:1702.01992* (2017), 17.

- [8] Daphne Camara Barcellos, Sergio Eduardo de Paiva Gonçalves, Melissa Aline da Silva, Graziela Ribeiro Batista, Patricia Rondon Pleffken, César Rogério Pucci, Alessandra Buhler Borges, and Carlos Rocha Gomes Torres. 2011. Prevalence of Chewing Side Preference in the Deciduous, Mixed and Permanent Dentitions. *Journal of Contemporary Dental Practice* 12, 5 (Sept. 2011), 339–342. <http://hdl.handle.net/11449/72646>
- [9] Abdelkareem Bedri, Richard Li, Malcolm Haynes, Raj Prateek Kosaraju, Ishaan Grover, Temiloluwa Prioleau, Min Yan Beh, Mayank Goel, Thad Starner, and Gregory Abowd. 2017. EarBit: Using Wearable Sensors to Detect Eating Episodes in Unconstrained Environments. *Proceedings of the ACM on interactive, mobile, wearable and ubiquitous technologies* 1, 3 (Sept. 2017), 37. doi:10.1145/3130902
- [10] Abdelkareem Bedri, Apoorva Verlekar, Edison Thomaz, Valerie Avva, and Thad Starner. 2015. Detecting Mastication: A Wearable Approach. In *Proceedings of the 2015 ACM on International Conference on Multimodal Interaction (ICMI '15)*. Association for Computing Machinery, New York, NY, USA, 247–250. doi:10.1145/2818346.2820767
- [11] Brooke M. Bell, Ridwan Alam, Nabil Alshurafa, Edison Thomaz, Abu S. Mondol, Kayla de la Haye, John A. Stankovic, John Lach, and Donna Spruijt-Metz. 2020. Automatic, wearable-based, in-field eating detection approaches for public health research: a scoping review. *npj Digital Medicine* 3, 1 (March 2020), 38. doi:10.1038/s41746-020-0246-2
- [12] Shengjie Bi, Tao Wang, Nicole Tobias, Josephine Nordrum, Shang Wang, George Halvorsen, Sougata Sen, Ronald Peterson, Kofi Odame, Kelly Caine, Ryan Halter, Jacob Sorber, and David Kotz. 2018. Auracle: Detecting Eating Episodes with an Ear-mounted Sensor. *Proc. ACM Interact. Mob. Wearable Ubiquitous Technol.* 2, 3 (Sept. 2018), 92:1–92:27. doi:10.1145/3264902
- [13] Mehrab Bin Morshed, Harish Kashyap Haresamudram, Dheeraj Bandaru, Gregory D. Abowd, and Thomas Ploetz. 2022. A Personalized Approach for Developing a Snacking Detection System using Earbuds in a Semi-Naturalistic Setting. In *Proceedings of the 2022 ACM International Symposium on Wearable Computers (ISWC '22)*. Association for Computing Machinery, New York, NY, USA, 11–16. doi:10.1145/3544794.3558469
- [14] Garvit Chugh, Indrajeet Ghosh, Sandip Chakraborty, and Suchetana Chakraborty. 2025. BiteSense: Earable-Based Inertial Sensing for Eating Behaviour Assessment. In *2025 IEEE International Conference on Pervasive Computing and Communications (PerCom)*. IEEE, Piscataway, NJ, USA, 110–120. doi:10.1109/PerCom64205.2025.00030
- [15] Jungman Chung, Jungmin Chung, Wonjun Oh, Yongkyu Yoo, Won Gu Lee, and Hyunwoo Bang. 2017. A glasses-type wearable device for monitoring the patterns of food intake and facial activity. *Scientific Reports* 7, 1 (Jan. 2017), 41690. doi:10.1038/srep41690
- [16] Yichen Dai, Ming Gao, Ruixuan Zhang, Yuefan Zhai, Kaiyan Cui, and Fu Xiao. 2025. Poster: IMU-Aided Speech Enhancement for COTS Earphones. In *Proceedings of the 31st Annual International Conference on Mobile Computing and Networking*. Association for Computing Machinery, New York, NY, USA, 1383–1385. <https://dl.acm.org/doi/10.1145/3680207.3765694>
- [17] Yimian Dai, Fabian Gieseke, Stefan Oehmcke, Yiquan Wu, and Kobus Barnard. 2021. Attentional feature fusion. In *Proceedings of the IEEE/CVF winter conference on applications of computer vision*. IEEE, Piscataway, NJ, USA, 3560–3569.
- [18] Berken Utku Demirel, Ting Dang, Khaldoon Al-Naimi, Fahim Kawsar, and Alessandro Montanari. 2024. Unobtrusive Air Leakage Estimation for Earables with In-ear Microphones. *Proc. ACM Interact. Mob. Wearable Ubiquitous Technol.* 7, 4 (Jan. 2024), 156:1–156:29. doi:10.1145/3631405
- [19] Peter Derleth, Eleftheria Georganti, Matthias Latzel, Gilles Courtois, Markus Hofbauer, Juliane Raether, and Volker Kuehnel. 2021. Binaural Signal Processing in Hearing Aids. *Seminars in Hearing* 42, 3 (Aug. 2021), 206–223. doi:10.1055/s-0041-1735176
- [20] S. Diernberger, O. Bernhardt, C. Schwahn, and B. Kordass. 2008. Self-reported chewing side preference and its associations with occlusal, temporomandibular and prosthodontic factors: results from the population-based Study of Health in Pomerania (SHIP-0). *Journal of Oral Rehabilitation* 35, 8 (2008), 613–620. doi:10.1111/j.1365-2842.2007.01790.x
- [21] S. F. Dworkin and L. LeResche. 1992. Research diagnostic criteria for temporomandibular disorders: review, criteria, examinations and specifications, critique. *Journal of Craniomandibular Disorders: Facial & Oral Pain* 6, 4 (1992), 301–355.
- [22] Muhammad Farooq and Edward Sazonov. 2015. Comparative testing of piezoelectric and printed strain sensors in characterization of chewing. In *2015 37th Annual International Conference of the IEEE Engineering in Medicine and Biology Society (EMBC)*. IEEE, Piscataway, NJ, USA, 7538–7541. doi:10.1109/EMBC.2015.7320136
- [23] Muhammad Farooq and Edward Sazonov. 2016. A Novel Wearable Device for Food Intake and Physical Activity Recognition. *Sensors* 16, 7 (July 2016), 1067. doi:10.3390/s16071067
- [24] Yang Gao, Ning Zhang, Honghao Wang, Xiang Ding, Xu Ye, Guanling Chen, and Yu Cao. 2016. iHear Food: Eating Detection Using Commodity Bluetooth Headsets. In *2016 IEEE First International Conference on Connected Health: Applications, Systems and Engineering Technologies (CHASE)*. IEEE, Piscataway, NJ, USA, 163–172. doi:10.1109/CHASE.2016.14
- [25] Michael Gunning and Ilias Tagkopoulos. 2025. A systematic review of data and models for predicting food flavor and texture. *Current Research in Food Science* 11 (Jan. 2025), 101127. doi:10.1016/j.crf.2025.101127
- [26] Shan He, Siying Li, Anindya Nag, Shilun Feng, Tao Han, Subhas Chandra Mukhopadhyay, and Warwick Powel. 2020. A comprehensive review of the use of sensors for food intake detection. *Sensors and Actuators A: Physical* 315 (Nov. 2020), 112318. doi:10.1016/j.sna.2020.112318
- [27] Dan Hendrycks and Kevin Gimpel. 2023. Gaussian Error Linear Units (GELUs). *arXiv preprint (2023)*, 10. arXiv:1606.08415 [cs.LG] <https://arxiv.org/abs/1606.08415>
- [28] Delwar Hossain, Tonmoy Ghosh, Masudul Haider Imtiaz, and Edward Sazonov. 2023. Ear canal pressure sensor for food intake detection. *Frontiers in Electronics* 4 (July 2023), 14. doi:10.3389/felec.2023.1173607 Publisher: Frontiers.
- [29] Changshuo Hu, Qiang Yang, Yang Liu, Tobias Röddiger, Kayla-Jade Butkow, Mathias Ciliberto, Adam Luke Pullin, Jake Stuchbury-Wass, Mahbub Hassan, Cecilia Mascolo, and Dong Ma. 2025. A Survey of Earable Technology: Trends, Tools, and the Road Ahead. arXiv:2506.05720 [cs.HC] <https://arxiv.org/abs/2506.05720>

- [30] Jie Hu, Li Shen, Samuel Albanie, Gang Sun, and Enhua Wu. 2019. Squeeze-and-Excitation Networks. (2019). arXiv:1709.01507 [cs.CV] <https://arxiv.org/abs/1709.01507>
- [31] Nick Hunn. 2024. *Introducing Bluetooth LE Audio*. Admitt Hub Ref Service PR. 412 pages.
- [32] Muhammad Huzaifah. 2017. Comparison of time-frequency representations for environmental sound classification using convolutional neural networks. *arXiv preprint arXiv:1706.07156* (2017), 5.
- [33] H. Jiang, C. Li, Z. Wang, J. Cao, X. Shi, J. Ma, and H. Liu. 2015. Assessment of osseous morphology of temporomandibular joint in asymptomatic participants with chewing-side preference. *Journal of Oral Rehabilitation* 42, 2 (2015), 105–112. doi:10.1111/joor.12240
- [34] H. Jiang, H. Liu, G. Liu, Z. Jin, L. Wang, J. Ma, and H. Li. 2015. Analysis of brain activity involved in chewing-side preference during chewing: an fMRI study. *Journal of Oral Rehabilitation* 42, 1 (2015), 27–33. doi:10.1111/joor.12224
- [35] Tamisa Ketmalasiri, Yu Yvonne Wu, Kayla-Jade Butkow, Cecilia Mascolo, and Yang Liu. 2024. IMChew: Chewing Analysis using Earphone Inertial Measurement Units. In *Proceedings of the Workshop on Body-Centric Computing Systems (BodySys '24)*. Association for Computing Machinery, New York, NY, USA, 29–34. doi:10.1145/3662009.3662022
- [36] Mohammad Imroze Khan, Bibhudendra Acharya, and Rahul Kumar Chaurasiya. 2022. iHearken: Chewing sound signal analysis based food intake recognition system using Bi-LSTM softmax network. *Computer Methods and Programs in Biomedicine* 221 (June 2022), 106843. doi:10.1016/j.cmpb.2022.106843
- [37] Sungtae Kim, Donghun Lee, and Jun Han. 2022. EarChew: towards identifying chewing side preference using earables. In *Proceedings of the 20th Annual International Conference on Mobile Systems, Applications and Services (MobiSys '22)*. Association for Computing Machinery, New York, NY, USA, 571–572. doi:10.1145/3498361.3538789
- [38] Diederik P. Kingma and Jimmy Ba. 2017. Adam: A Method for Stochastic Optimization. arXiv:1412.6980 [cs.LG] <https://arxiv.org/abs/1412.6980>
- [39] C. Knapp and G. Carter. 1976. The generalized correlation method for estimation of time delay. *IEEE Transactions on Acoustics, Speech, and Signal Processing* 24, 4 (1976), 320–327. doi:10.1109/TASSP.1976.1162830
- [40] Takumi Kondo, Hidekazu Shiro, Anna Yokokubo, and Guillaume Lopez. 2019. Optimized Classification Model for Efficient Recognition of Meal-Related Activities in Daily Life Meal Environment. In *2019 Joint 8th International Conference on Informatics, Electronics & Vision (ICIEV) and 2019 3rd International Conference on Imaging, Vision & Pattern Recognition (icIVPR)*. IEEE, Piscataway, NJ, USA, 146–151. doi:10.1109/ICIEV.2019.8858526
- [41] Joo-Young Lee, Eun-Song Lee, Gyung-Min Kim, Hoi-In Jung, Jeong-Woo Lee, Ho-Keun Kwon, and Baek-Il Kim. 2019. Unilateral Mastication Evaluated Using Asymmetric Functional Tooth Units as a Risk Indicator for Hearing Loss. *Journal of Epidemiology* 29, 8 (Aug. 2019), 302–307. doi:10.2188/jea.JE20180052
- [42] Zhe Li, Ang Li, Chong Guo, Pengxuan Sun, Haotian Zhu, and Tianqi Peng. 2024. IMU-Based CWT and Whitening-Aided for Human Activity Recognition. In *Proceedings of the 2024 8th International Conference on Advances in Image Processing (ICAIP) (ICAIP '24)*. Association for Computing Machinery, New York, NY, USA, 81–86. doi:10.1145/3702370.3702378
- [43] Jian Liang, Ran He, and Tieniu Tan. 2025. A Comprehensive Survey on Test-Time Adaptation Under Distribution Shifts. *International Journal of Computer Vision* 133, 1 (Jan. 2025), 31–64. doi:10.1007/s11263-024-02181-w
- [44] Jindong Liu, Edward Johns, Louis Atallah, Claire Pettitt, Benny Lo, Gary Frost, and Guang-Zhong Yang. 2012. An Intelligent Food-Intake Monitoring System Using Wearable Sensors. In *2012 Ninth International Conference on Wearable and Implantable Body Sensor Networks*. IEEE, Piscataway, NJ, USA, 154–160. doi:10.1109/BSN.2012.11
- [45] Paulo Lopez-Meyer, Oleksandr Makeyev, Stephanie Schuckers, Edward L. Melanson, Michael R. Neuman, and Edward Sazonov. 2010. Detection of Food Intake from Swallowing Sequences by Supervised and Unsupervised Methods. *Annals of Biomedical Engineering* 38, 8 (Aug. 2010), 2766–2774. doi:10.1007/s10439-010-0019-1
- [46] Roya Lotfi, George Tzanetakis, Rasit Eskicioglu, and Pourang Irani. 2020. A comparison between audio and IMU data to detect chewing events based on an earable device. In *Proceedings of the 11th Augmented Human International Conference (AH '20)*. Association for Computing Machinery, New York, NY, USA, 1–8. doi:10.1145/3396339.3396362
- [47] José López-Cedrún, Urbano Santana-Mora, María Pombo, Amaya Pérez Del Palomar, Víctor Alonso De la Peña, María Jesús Mora, and Urbano Santana. 2017. Jaw biodynamic data for 24 patients with chronic unilateral temporomandibular disorder. *Scientific Data* 4, 1 (Nov. 2017), 170168. doi:10.1038/sdata.2017.168
- [48] Kushagra Maini and Anterpreet Dua. 2025. Temporomandibular Syndrome. In *StatPearls*. StatPearls Publishing, Treasure Island (FL). <http://www.ncbi.nlm.nih.gov/books/NBK551612/>
- [49] Jordi Martinez-Gomis, Mar Lujan-Climent, Sara Palau, Josep Bizar, Juan Salsench, and Maria Peraire. 2009. Relationship between chewing side preference and handedness and lateral asymmetry of peripheral factors. *Archives of Oral Biology* 54, 2 (Feb. 2009), 101–107. doi:10.1016/j.archoralbio.2008.09.006
- [50] S. T. Mc Donnell, M. P. Hector, and A. Hannigan. 2004. Chewing side preferences in children. *Journal of Oral Rehabilitation* 31, 9 (2004), 855–860. doi:10.1111/j.1365-2842.2004.01316.x
- [51] Akihiro Nakamura, Hiroshi Mineno, Masafumi Nishimura, Takato Saito, Daizo Ikeda, and Ken Ohta. 2020. Automatic Detection of the Chewing Side Using Two-channel Recordings under the Ear. In *2020 IEEE 2nd Global Conference on Life Sciences and Technologies (LifeTech)*. IEEE, Piscataway, NJ, USA, 82–83. doi:10.1109/LifeTech48969.2020.1570618941
- [52] Akihiro Nakamura, Ken Ohta, Takato Saito, Hiroshi Mineno, Daizo Ikeda, and Masafumi Nishimura. 2020. Automatic Detection of Chewing and Swallowing Using Hybrid CTC/Attention. In *2020 IEEE 9th Global Conference on Consumer Electronics (GCCE)*. IEEE, Piscataway, NJ, USA, 810–812.

- doi:10.1109/GCCE50665.2020.9292024
- [53] Akihiro Nakamura, Takato Saito, Daizo Ikeda, Ken Ohta, Hiroshi Mineno, and Masafumi Nishimura. 2021. Automatic Detection of Chewing and Swallowing Using Multichannel Sound Information. In *2021 IEEE 3rd Global Conference on Life Sciences and Technologies (LifeTech)*. IEEE, Piscataway, NJ, USA, 173–175. doi:10.1109/LifeTech52111.2021.9391873
- [54] Engineering National Academies of Sciences, Health and Medicine Division, Board on Health Care Services, Board on Health Sciences Policy, Committee on Temporomandibular Disorders (TMDs): From Research Discoveries to Clinical Treatment, Olivia Yost, Cathy T. Liverman, Rebecca English, Sean Mackey, and Enriqueta C. Bond. 2020. Prevalence, Impact, and Costs of Treatment for Temporomandibular Disorders. In *Temporomandibular Disorders: Priorities for Research and Care*. National Academies Press (US), Washington DC, USA. <https://www.ncbi.nlm.nih.gov/books/NBK557996/>
- [55] Jun Nishimura and Tadahiro Kuroda. 2008. Eating habits monitoring using wireless wearable in-ear microphone. In *2008 3rd International Symposium on Wireless Pervasive Computing*. IEEE, Piscataway, NJ, USA, 130–132. doi:10.1109/ISWPC.2008.4556181
- [56] National Institute of Dental and Craniofacial Research. 2018. Facial Pain. <https://web.archive.org/web/20180422220838/https://www.nidcr.nih.gov/research/data-statistics/facial-pain>
- [57] University of Leeds. 2025. Improving outcomes for chronic orofacial pain including temporomandibular disorders – The TMD study. <https://medicinehealth.leeds.ac.uk/dentistry-research-innovation/dir-record/research-projects/1764/improving-outcomes-for-chronic-orofacial-pain-including-temporomandibular-disorders-the-tmd-study> [Accessed: December 23, 2025].
- [58] Vasileios Papanagiotou, Christos Diou, Lingchuan Zhou, Janet van den Boer, Monica Mars, and Anastasios Delopoulos. 2017. A Novel Chewing Detection System Based on PPG, Audio, and Accelerometry. *IEEE Journal of Biomedical and Health Informatics* 21, 3 (May 2017), 607–618. doi:10.1109/JBHI.2016.2625271
- [59] Younjung Park, Sora Yoon, Joon-Ho Yoon, and Jin-Joo Yoo. 2025. Association between temporomandibular disorders and mental and behavioural disorders - a nationwide population-based cross-sectional study. *Clinical Oral Investigations* 29, 5 (April 2025), 234. doi:10.1007/s00784-025-06324-2
- [60] Adam Paszke, Sam Gross, Francisco Massa, Adam Lerer, James Bradbury, Gregory Chanan, Trevor Killeen, Zeming Lin, Natalia Gimelshein, Luca Antiga, et al. 2019. Pytorch: An imperative style, high-performance deep learning library. *Advances in neural information processing systems* 32 (2019).
- [61] Sebastian Paßler and Wolf-Joachim Fischer. 2011. Food Intake Activity Detection Using a Wearable Microphone System. In *2011 Seventh International Conference on Intelligent Environments*. IEEE, Piscataway, NJ, USA, 298–301. doi:10.1109/IE.2011.9
- [62] Miguel Ramón Pecci-Lloret, Carmen María García-Sampedro, Julia Guerrero-Gironés, and Emilio López-Jiménez. 2025. Observational Study: Preliminary Evaluation of Nostril Narrowing in Relation to Unilateral Mastication. *Journal of Clinical Medicine* 14, 4 (Jan. 2025), 1319. doi:10.3390/jcm14041319
- [63] Dang Thoai Phan. 2025. Comparison Performance of Spectrogram and Scalogram as Input of Acoustic Recognition Task. In *Advances in Information and Communication*. Springer Nature Switzerland, 660–673. doi:10.1007/978-3-031-84457-7_41
- [64] J.M.C. Po, J.A. Kieser, L.M. Gallo, A.J. Tésenyi, P. Herbison, and M. Farella. 2011. Time-Frequency Analysis of Chewing Activity in the Natural Environment. *Journal of Dental Research* 90, 10 (Oct. 2011), 1206–1210. doi:10.1177/0022034511416669 Publisher: SAGE Publications Inc.
- [65] Sebastian Paßler and Wolf-Joachim Fischer. 2014. Food Intake Monitoring: Automated Chew Event Detection in Chewing Sounds. *IEEE Journal of Biomedical and Health Informatics* 18, 1 (Jan. 2014), 278–289. doi:10.1109/JBHI.2013.2268663
- [66] Ali Jamal Abdul Razzaq and Zaid Dewachi. 2023. Three-dimensional of lingual arch form and creation of templates in Iraqi normal occlusion. *Journal of Orthodontic Science* 12, 1 (Nov. 2023), 81. doi:10.4103/jos.jos_119_22
- [67] Tobias Röddiger, Michael Küttner, Philipp Lepold, Tobias King, Dennis Moschina, Oliver Bagge, Joseph A. Paradiso, Christopher Clarke, and Michael Beigl. 2025. OpenEarable 2.0: Open-Source Earphone Platform for Physiological Ear Sensing. *Proc. ACM Interact. Mob. Wearable Ubiquitous Technol.* 9, 1, Article 16 (March 2025), 33 pages. doi:10.1145/3712069
- [68] B. Rovira-Lastra, E. I. Flores-Orozco, R. Ayuso-Montero, M. Péraire, and J. Martinez-Gomis. 2016. Peripheral, functional and postural asymmetries related to the preferred chewing side in adults with natural dentition. *Journal of Oral Rehabilitation* 43, 4 (2016), 279–285. doi:10.1111/joor.12369
- [69] Tobias Röddiger, Christopher Clarke, Paula Breitling, Tim Schneegans, Haibin Zhao, Hans Gellersen, and Michael Beigl. 2022. Sensing with Earables: A Systematic Literature Review and Taxonomy of Phenomena. *Proc. ACM Interact. Mob. Wearable Ubiquitous Technol.* 6, 3 (Sept. 2022), 1–57. doi:10.1145/3550314
- [70] Tobias Röddiger, Christopher Clarke, Daniel Wolfram, Matthias Budde, and Michael Beigl. 2021. EarRumble: Discreet Hands- and Eyes-Free Input by Voluntary Tensor Tympani Muscle Contraction. In *Proceedings of the 2021 CHI Conference on Human Factors in Computing Systems (CHI '21)*. Association for Computing Machinery, New York, NY, USA, 1–14. doi:10.1145/3411764.3445205
- [71] Mark Sandler, Andrew G. Howard, Menglong Zhu, Andrey Zhmoginov, and Liang-Chieh Chen. 2018. Inverted Residuals and Linear Bottlenecks: Mobile Networks for Classification, Detection and Segmentation. *CoRR* abs/1801.04381 (2018), 14. arXiv:1801.04381 <http://arxiv.org/abs/1801.04381>
- [72] Urbano Santana-Mora, José López-Cedrún, María J. Mora, Xosé L. Otero, and Urbano Santana-Penín. 2013. Temporomandibular Disorders: The Habitual Chewing Side Syndrome. *PLOS ONE* 8, 4 (April 2013), e59980. doi:10.1371/journal.pone.0059980
- [73] Edward S. Sazonov and Juan M. Fontana. 2012. A Sensor System for Automatic Detection of Food Intake Through Non-Invasive Monitoring of Chewing. *IEEE Sensors Journal* 12, 5 (May 2012), 1340–1348. doi:10.1109/JSEN.2011.2172411
- [74] Michele Scarpiniti, Raffaele Parisi, and Yong-Cheol Lee. 2023. A Scalogram-based CNN approach for audio classification in construction sites. *Applied Sciences* 14, 1 (2023), 90.

- [75] Eric Schiffman, Richard Ohrbach, Edmond Truelove, John Look, Gary Anderson, Jean-Paul Goulet, Thomas List, Peter Svensson, Yoly Gonzalez, Frank Lobbezoo, Ambra Michelotti, Sharon L. Brooks, Werner Ceusters, Mark Drangsholt, Dominik Ettlin, Charly Gaul, Louis J. Goldberg, Jennifer A. Haythornthwaite, Lars Hollender, Rigmor Jensen, Mike T. John, Antoon De Laat, Reny de Leeuw, William Maixner, Marylee van der Meulen, Greg M. Murray, Donald R. Nixdorf, Sandro Palla, Arne Petersson, Paul Pionchon, Barry Smith, Corine M. Visscher, Joanna Zakrzewska, and Samuel F. Dworkin. 2014. Diagnostic Criteria for Temporomandibular Disorders (DC/TMD) for Clinical and Research Applications: Recommendations of the International RDC/TMD Consortium Network* and Orofacial Pain Special Interest Group†. [doi:10.11607/jop.1151](https://doi.org/10.11607/jop.1151)
- [76] Steven J. Scrivani, David A. Keith, and Leonard B. Kaban. 2008. Temporomandibular Disorders. *New England Journal of Medicine* 359, 25 (Dec. 2008), 2693–2705. [doi:10.1056/NEJMra0802472](https://doi.org/10.1056/NEJMra0802472)
- [77] Yuko Shikama, Kaede Matsuyama, Hiroko Kobayashi, Takahiro Suzuki, Aiji Sato-Boku, Motoko Takaoka, and Yasuyuki Shibuya. 2024. Texture analysis of food samples used for the evaluation of masticatory function. *Cureus* 16, 4 (2024), 13.
- [78] Masaki Shuzo, Shintaro Komori, Tomoko Takashima, Guillaume Lopez, Seiji Tatsuta, Shintaro Yanagimoto, Shin'ichi Warisawa, Jean-Jacques Delaunay, and Ichiro Yamada. 2010. Wearable Eating Habit Sensing System Using Internal Body Sound. *Journal of Advanced Mechanical Design, Systems, and Manufacturing* 4, 1 (2010), 158–166. [doi:10.1299/jamdsm.4.158](https://doi.org/10.1299/jamdsm.4.158)
- [79] Michel H. Steenks, Jens Christoph Türp, Dent Habil, and Anton de Wijer. 2018. Temporomandibular Disorders Axis I in Clinical and Research Settings: A Critical Appraisal. [doi:10.11607/ofph.1704](https://doi.org/10.11607/ofph.1704)
- [80] Alina Surmacka Szczesniak. 1963. Classification of Textural Characteristics^a. *Journal of Food Science* 28, 4 (July 1963), 385–389. [doi:10.1111/j.1365-2621.1963.tb00215.x](https://doi.org/10.1111/j.1365-2621.1963.tb00215.x)
- [81] Daniel Talmaceanu, Lavinia Manuela Lenghel, Nicolae Bolog, Mihaela Hedesiu, Smaranda Buduru, Horatiu Rotar, Mihaela Baciut, and Grigore Baciut. 2018. Imaging modalities for temporomandibular joint disorders: an update. *Clujul Medical* 91, 3 (July 2018), 280–287. [doi:10.15386/cjmed-970](https://doi.org/10.15386/cjmed-970)
- [82] Mingxing Tan and Quoc Le. 2019. EfficientNet: Rethinking Model Scaling for Convolutional Neural Networks. In *Proceedings of the 36th International Conference on Machine Learning (Proceedings of Machine Learning Research, Vol. 97)*, Kamalika Chaudhuri and Ruslan Salakhutdinov (Eds.). PMLR, 6105–6114. <https://proceedings.mlr.press/v97/tan19a.html>
- [83] Kazuhiro Taniguchi, Hisashi Kondo, Toshiya Tanaka, and Atsushi Nishikawa. 2018. Earable RCC: Development of an Earphone-Type Reliable Chewing-Count Measurement Device. *Journal of Healthcare Engineering* 2018, 1 (2018), 6161525. [doi:10.1155/2018/6161525](https://doi.org/10.1155/2018/6161525)
- [84] Shreyasi Tiwari, Supriya Nambiar, and Bhaskaran Unnikrishnan. 2017. Chewing Side Preference - Impact on Facial Symmetry, Dentition and Temporomandibular Joint and its Correlation with Handedness. *Journal of Orofacial Sciences* 9, 1 (June 2017), 22. [doi:10.4103/jofs.jofs_74_16](https://doi.org/10.4103/jofs.jofs_74_16)
- [85] Hiyori Tsuji, Takashi Amesaka, Sho Usuda, Wataru Muraoka, Taneaki Nakagawa, and Yuta Sugiura. 2025. HearTMD: Detection of Temporomandibular Disorder Using Hearables. In *Adjunct Proceedings of the 38th Annual ACM Symposium on User Interface Software and Technology (UIST Adjunct '25)*. Association for Computing Machinery, New York, NY, USA, 1–3. [doi:10.1145/3746058.3758416](https://doi.org/10.1145/3746058.3758416)
- [86] Tri Vu, Feng Lin, Nabil Alshurafa, and Wenyao Xu. 2017. Wearable Food Intake Monitoring Technologies: A Comprehensive Review. *Computers* 6, 1 (March 2017), 4. [doi:10.3390/computers6010004](https://doi.org/10.3390/computers6010004)
- [87] Shuangquan Wang, Gang Zhou, Amanda Watson, Lei Xie, Minglong Sun, and Woosub Jung. 2021. Wearable motion sensor-based chewing side detection. *Smart Health* 21 (July 2021), 100205. [doi:10.1016/j.smhl.2021.100205](https://doi.org/10.1016/j.smhl.2021.100205)
- [88] Yo Yamasaki, Rika Kuwatsuru, Yoshihiro Tsukiyama, Hiroshi Matsumoto, Kyosuke Oki, and Kiyoshi Koyano. 2015. Objective Assessment of Actual Chewing Side by Measurement of Bilateral Masseter Muscle Electromyography. *Archives of Oral Biology* 60, 12 (Dec. 2015), 1756–1762. [doi:10.1016/j.archoralbio.2015.09.010](https://doi.org/10.1016/j.archoralbio.2015.09.010)
- [89] Adrian Ujin Yap, Sunghae Kim, Byeong-min Lee, Jung Hwan Jo, and Ji Woon Park. 2024. Sleeping and waking-state oral behaviors in TMD patients: their correlates with jaw functional limitation and psychological distress. *Clinical Oral Investigations* 28, 6 (May 2024), 332. [doi:10.1007/s00784-024-05730-2](https://doi.org/10.1007/s00784-024-05730-2)
- [90] Haibin Zhao, Tobias Röddiger, Yufei Feng, and Michael Beigl. 2024. Fit2Ear: Generating Personalized Earplugs from Smartphone Depth Camera Images. In *Companion of the 2024 on ACM International Joint Conference on Pervasive and Ubiquitous Computing (UbiComp '24)*. Association for Computing Machinery, New York, NY, USA, 679–684. [doi:10.1145/3675094.3680525](https://doi.org/10.1145/3675094.3680525)
- [91] Grzegorz Zieliński, Beata Pająk-Zielińska, and Michał Ginszt. 2024. A Meta-Analysis of the Global Prevalence of Temporomandibular Disorders. *Journal of Clinical Medicine* 13, 5 (Jan. 2024), 1365. [doi:10.3390/jcm13051365](https://doi.org/10.3390/jcm13051365)

A Appendix A: Pre-Questionnaire

The pre-questionnaire collected basic demographic and dental information from all participants. Note that the dental diagram referenced in the questionnaire is not included here due to copyright restrictions.

Gender: Please select your gender.

Response options: Male; Female; Diverse; Prefer not to say.

Age: Please enter your age in years.

Response options: Open Answer.

Handedness: Are you left-handed or right-handed?

Response options: Left-handed; Right-handed.

Missing Teeth: Are you missing any teeth that have not been replaced with replacement materials or implants (i.e., do you have gaps in your teeth)? Missing wisdom teeth are excluded!

Response options: Yes; No.

Note: People were excluded from the study if they answered *Yes*.

Wisdom Teeth: Do you have your wisdom teeth?

Response options: Yes; Yes, but not erupted; No; Partially or Partially erupted (Please mark accordingly in the diagram on the accompanying paper sheet).

Teeth Repairs: Do you have fillings, crowns, implants, or other dental restorations? If yes, please indicate the affected teeth in the diagram on the accompanying paper sheet and specify the material used for each tooth (if known).

Response options: Yes (Please mark accordingly in the diagram); No.

Dental Malocclusions: Do you have any other dental malocclusions (e.g., overbite or underbite)? Please list them and briefly describe if necessary.

Response options: Open Answer.

B Appendix B: Post-Questionnaire

We reviewed the existing literature for questionnaires assessing the usability and acceptability of wearing devices while eating, but identified only a single relevant example [44]. This served as an initial reference point, although the final questionnaire was developed specifically for the present study.

Usability

All items were answered on a 7-point Likert scale (*1 = Totally Disagree, 7 = Totally Agree*).

Instructions: Please answer the questions on the usability and comfort of the chewing detection with earables below.

- (1) The earables were comfortable to wear throughout the study.
- (2) The earables fit my ears well.
- (3) Wearing the earables did not cause any pain or irritation.
- (4) Movements of the earables during chewing created distracting noises in my ears.
- (5) The earables did not interfere with my eating.
- (6) The earables stayed securely in place while I moved or chewed.
- (7) I felt that the earables were suitable for chewing-side detection.
- (8) Do you have any additional comments or suggestions regarding the comfort or usability of the earables for chewing-side detection? (*Open Answer*)

Acceptability

All items were answered on a 7-point Likert scale (*1 = Very Uncomfortable, 7 = Very Comfortable*).

Instructions: Please answer the questions on wearing the earables for chewing side detection in different situations.

Leading Question: I would feel comfortable wearing the earables for chewing-side detection in the following places and situations:

- (1) At home (alone)
- (2) At home (with family)
- (3) At home (with friends)
- (4) In the dining hall (alone)
- (5) In the dining hall (with family)
- (6) In the dining hall (with friends)
- (7) At a fast-food place (alone)
- (8) At a fast-food place (with family)
- (9) At a fast-food place (with friends)
- (10) In a café (alone)
- (11) In a café (with family)
- (12) In a café (with friends)
- (13) In a restaurant (alone)
- (14) In a restaurant (with family)

- (15) In a restaurant (with friends)
- (16) Do you have any additional comments or suggestions about the comfort of wearing the earables during chewing side detection in different situations? (*Open Answer*)

C Appendix C: Food Selection Prompt

Each of the LLMs (GPT-5, Gemini 3, and Claude Sonnet 4.5) was given the following prompt for estimating the brittleness and chewiness of the chosen foods.

```
You are analyzing food texture using two parameters: Brittleness (the force with which a food fractures, linked to hardness and cohesiveness) and Chewiness (the energy required to chew a food until it can be swallowed, linked to hardness, cohesiveness, and elasticity).

Task: For each of the following foods, (1) provide a short description of its brittleness and chewiness, and (2) rate both parameters on a scale from 1 (very low) to 10 (very high).

Foods: Almonds, Apple, Banana, Bread, Chewing Gum, Gummy Bears, Lettuce, Potato Chips, Semi-Hard Cheese, Snack Pretzels.

Output format: First give the descriptions (grouped under each food). Then present ratings as Python lists in this structure:

foods = ["Almonds", "Apple", "Banana", "Bread", "Chewing Gum", "Gummy Bears", "Lettuce", "Potato Chips", "Semi-Hard Cheese", "Snack Pretzels"]
brittleness = [ ... ] # brittleness ratings
chewiness = [ ... ] # chewiness ratings
```

D Appendix D: Bowl Characteristics

For the study, a bowl was ordered from Dean and David³. To align with the study design, a *Mix Your Own* bowl was selected, allowing participants to configure their meal within predefined options. This ensured both diversity in composition and overall comparability across participants. The available choices were as follows:

- (1) Base: salad and rice (jasmine fragrant rice OR quinoa wholegrain rice)
- (2) Crunchy topping: croutons OR crunchy onions OR peanuts OR walnuts OR sunflower seeds
- (3) Hard vegetable: cucumber OR carrot OR bell pepper
- (4) Soft vegetable: mango OR beetroot OR tomato
- (5) Protein: chicken OR beef OR salmon OR halloumi OR vegetarian chicken OR falafel
- (6) Dressing: choice of participant

³Official Website

E Appendix E: Baseline Random Forest Specifications

The Random Forest (RF) classifier used as a baseline closely replicated the models used in Ketmalasiri et al. [35] and Lotfi et al. [46] for chewing detection. The exact specifications are reported below.

Feature Extraction

- Time-domain features: Mean, Variance, Power
- Frequency-domain features: Spectral Centroid, Mel-Frequency Cepstral Coefficients (MFCCs).
- All features were Z -standardized using per-feature training mean and standard deviation. Frequency-domain features were extracted using a Fourier transform with the following sensor-specific parameters:

Sensor	N_{FFT}	hop_length	N_{MFCC}	N_{MELS}
Microphones	1024	128	13	40
Bone Conduction Microphone	256	64	12	20
IMU	128	32	12	20
PPG	64	16	12	20
Pressure Sensor	128	32	12	20

Random Forest Model Configuration

- Ensemble
 - n_estimators: 100
 - bootstrap: True
 - max_samples: 0.8
 - random_state: 42
- Tree Structure
 - max_depth: 10
 - min_samples_split: 20
 - min_samples_leaf: 10
 - max_features: sqrt
- Regularization and Class Balancing
 - min_impurity_decrease: 0.0
 - ccp_alpha: 0.01
 - class_weight: balanced